

Incorporating observed fire severity in refined emissions estimates for boreal and temperate forest fires in the carbon budget model CBM-CFS3

Dan K. Thompson¹, Ellen Whitman², Hafer Mark³, Oleksandra Hararuk², Chelene Hanes¹, Vinicius Manvailer Goncalves³, and Ben Hudson³

¹Natural Resources Canada, Canadian Forest Service, Great Lakes Forestry Centre, Sault Ste. Marie, Canada

²Natural Resources Canada, Canadian Forest Service, Northern Forestry Centre, Edmonton, Canada

³Natural Resources Canada, Canadian Forest Service, Pacific Forestry Centre, Victoria, Canada

Abstract. Among the many natural disturbances that affect Canada's boreal and temperate forest biomes, wildfire has the greatest impact on forest productivity, landscape structure, timber supply and greenhouse gas emissions. Current representations of fire impact on forest carbon stocks is limited to a single parameterization of fire severity (i.e. the fate of biomass including consumption) that assumes only high severity fires, despite a large evidence base of widespread mixed-severity boreal wildfire. This paper describes a sub-model, termed FireDMs (Fire Disturbance Matrix: severity), of the National Forest Carbon Monitoring Accounting and Reporting System for Canada (NFC-MARS). In this sub-model, field measurements of biomass consumption are related to satellite-derived burn severity maps and are interpreted from a fire physics and ecology perspective to derive estimates of the forest greenhouse gas fluxes in the immediate aftermath of fires. The sub-model also quantifies fire-killed by uncombusted biomass as a set of distinct pools. Model outputs indicate total direct carbon emissions range from a 11 t C/ha in Boreal Shield West forests of Saskatchewan following low severity fire to over 60 t C/ha in Pacific Maritime forests of British Columbia under high severity fire. The existing approach to emissions in NFC-MARS yields regional CO₂e emissions that are 10-25 percent higher than this new method, owing to lower overall canopy consumption with mixed-severity fires, which is only partially offset by increased estimates forest floor consumption in this new approach. Comparisons against directly observed fire plume emissions ratios as well as against annualized carbon emissions for Canada's 2023 fire season show good model agreement with observations.

. His Majesty the King in Right of Canada as represented by the Minister of Natural Resources Canada. This work is distributed under the Creative Commons Attribution 4.0 License.

1 Introduction

Wildfire is on par with insects as the largest stand-replacing disturbance process in Canada's forest, impacting ~1–3 Mha of Canada's 367 Mha forested area in a typical year (Hanes et al., 2019). In Canada's reliable 54-year burned area record, ten

years have exceeded 4 Mha of burned area (or approximately 1% of Canada's forest area) (Skakun et al., 2022). The 2023 fire season in Canada burned a remarkable 15 Mha owing to extreme drought, severe fire weather conditions, and a prolonged fire season length (Jain et al., 2024).

Of this, publicly-owned managed forest under long or short-term tenure accounts for 23% of the area burned between 1972 and 2024; publicly-owned managed forest under long-term license to private timber companies forms 40% of Canada's forest area (Stinson et al., 2019). Privately-owned forest constitutes only 6% of the forest area, but only 0.5% of area burned. The remainder of the forest area burned in Canada being a mix of formally protected areas, remote unmanaged forest, Indigenous reserve lands and other uses without large-scale harvesting. Managed northern forest areas adjacent to communities have historically shown some meaningful local fire suppression effects with a bias towards older forest nearby boreal forest communities in Canada, though the effect is largely limited to a 25 km radius between these widely dispersed communities (Parisien et al., 2020). More southern boreal forest with extensive suppression activities has historically seen evidence of a reduction in observed vs potential area burned (Cumming, 2005) though this effect has likely been erased given the increasing frequency of extreme burning conditions Wang et al. (2023) and corresponding record area burned (Jain et al., 2024).

Burned area in Canada is dominated by a relatively small number of very large fires, with 3% of fires constituting 97% of the burned area (Stocks et al., 2002). Lightning-caused fires account for approximately half of all ignitions and approximately 80% of burned area, but no distinction is made between human and lightning ignition for forest sector GHG reporting purposes. Annual burned area mapping for GHG reporting in Canada is conducted using a composite of satellite and aerial mapping at 30 metre resolution; the relatively small number of large fires, and their slow vegetation regeneration (White et al., 2017) allows for reliable mapping using multi-spectral imagery such as Landsat within one year of the fire (Whitman et al., 2018).

Canada reports on GHG emission and removals from the forest sector in Canada's National GHG Inventory Report (NIR). Carbon stocks and stock changes are modelled using CBM-CFS3 (Kurz et al., 2009) parameterized and driven by spatial and non-spatial data describing forest inventory, annual yield and disturbance (Stinson et al., 2011). Following international good practice guidance to focus on human-caused emissions in NIRs, Canada focuses emission reporting on managed forest lands, which make up approximately 225 Mha of Canada's 367 Mha total forest area. In CBM-CFS3, forest inventory is represented by spatially referenced stand lists representing large homogeneous stands that fall within spatial units (e.g. forest management areas) and broad regions called Reconciliation Units (RU) that are the intersection of ecozones with provincial/territorial boundaries (Kurz et al., 2002). Within CBM-CFS3 precisely mapped burned areas (Hall et al., 2020) are summarized at the level of spatial units and applied randomly to stands within that unit. Years with larger burned areas will improve the representative nature of random stands being assigned fire disturbance within a year, as a wider variety of stand types will be selected. Furthermore, large, drought-driven fire years such as 2023 have been observed to burn at more equal rates across the diversity of local ecosite flammability (Parks et al., 2018; Whitman et al., 2024) and thus provides an ideal test case for assessing changes in emissions estimates for a spatially referenced system. Importantly, these years with very large area burned still show a similar natural range in variability of burn severity (Whitman et al., 2018).

CBM-CFS3 currently assesses fire impacts to carbon pools only as representing high-severity fire, which is the most common of the three severity classes (low, moderate, and high) used for assessing of burned forest in Canada (Hall et al., 2008b) and

the conterminous US (Eidenshink et al., 2007). Currently, biomass consumption estimates are based on the assumption of complete crown mortality, with additional biomass consumption following a spatially-referenced aggregated estimate at the RU of annualized drought conditions. Quantification of the change in carbon stock in CBM-CFS3 is made via a “Disturbance Matrix” (hereafter referred to as a DM) which is simply a matrix of the proportional mass flux of carbon (12 g/mol elemental carbon, not biomass units) between each pair of pools in the model for a site experiencing a given disturbance. This proportional mass flux is independent of the size of the C pool. Pools in the DM include all the above and below-ground pools tracked in CBM-CFS3, as well as an atmospheric sink pool. Importantly, unlike emissions-only fire models commonly used in air quality modelling in Canada (Chen et al., 2019), DM definitions in CBM-CFS3 also track the transfer of live biomass to dead, but still uncombusted pools, such as the transfer from live stemwood pools (which are killed but not burned) to standing deadwood, also known as snags.

In Canada’s forests, a combination of climate, disturbance history, soils, and less frequently topographic variables determine leading tree species; at local scales (1–100 ha), tree species composition plays a major role in determining ecosystem susceptibility to fire (Bernier et al., 2016) where older, conifer-dominated forests burn at very high rates relative to adjacent deciduous or mixed stands. Even when deciduous and mixed forests burn at rates more similar to older conifer stands during large drought-driven fire years (Parks et al., 2014), they do so at consistently lower severity compared to all but the most xeric conifer forests (Whitman et al., 2018). Thus, important local biases in fire activity and severity towards older and moderate to poorly-drained forests are not resolved in the spatially-referenced CBM-CFS3 when a uniform fire severity is applied.

To support recent advances in operational burn severity mapping for Canada (Whitman et al., 2020) alongside multi-decade reliable burned area records that provide certainty on fire start and end dates (Guindon et al., 2014; Hall et al., 2020), this paper describes a local scale (30-m) method for defining a per-pixel proportional carbon flux estimate via a locally calculated fire DM. In this document, we outline the evidence-based fire Disturbance Matrices (DM) updated and designed for a planned, spatially-explicit update to the CBM-CFS3, anchored in a three severity class paradigm. These fire carbon flux models are built from a blend of aggregated field data linked to remotely sensed severity, as well as insights from fire physics and experimental fires. Key knowledge gaps are also highlighted, with interim solutions presented until further quantification can be done in field studies, such as from further wildfire observations, experimental fires, or prescribed fires.

Simplified fire DMs (i.e. a scalar reduction on 100% mortality assumption across all DM components) have been used in valuable scenario exercises using a spatial explicit version of CBM-CFS3 for assessment of future fire and harvest scenarios (Smyth et al., 2022). The algorithm development shown here provides an important data-driven and regionally-adjusted framework that better reflects the ecological nuances of moderate and low-severity fire across Canada’s diverse ecozones.

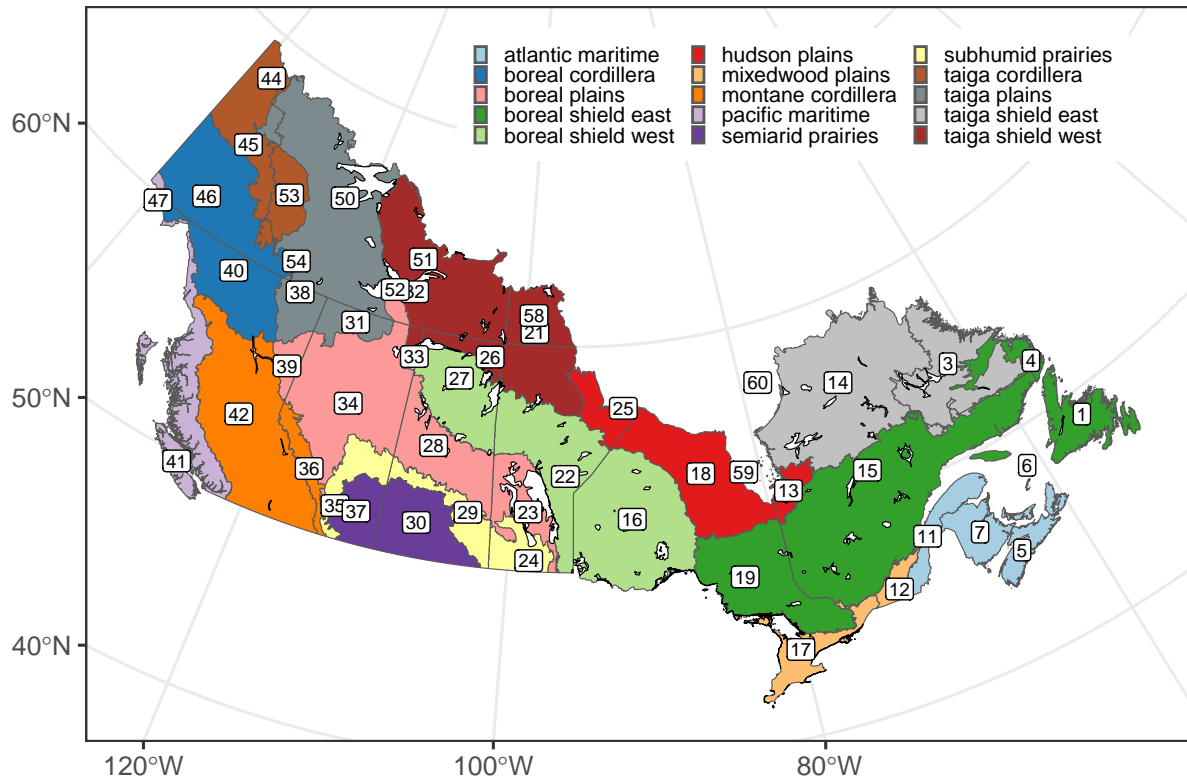


Figure 1. Reconciliation Units used in the CBM-CFS3 framework.

2 Methods

2.1 Carbon Modelling

2.2 Carbon Modelling Spatial Units

Carbon reporting in Canada's forests is broken down by Reconciliation Unit (RU), which is the intersection of terrestrial ecozones and provincial/territorial boundaries, as shown in Figure 1. Forest carbon stocks in Canada are influenced by species composition, age class distribution, natural disturbance history, human-influenced management regime and climatic variables, among other factors, which are well-represented by the RU framework supporting Canada's NIR. Due to the current spatial imprecision of certain key model data (e.g. deforestation rates), analysis finer than the RU-level tends to misrepresent regional-variation in emission estimates. ## Biomass pools of the CBM-CFS3 Model

The carbon pools represented in CBM-CFS3 can be broadly categorized as live biomass, dead organic matter (DOM) and soil carbon and are described in detail in Kurz et al. (2009). Key components that interact most with wildfire are summarized

Table 1. Key components of the CBM-CFS3 model relevant to fire behaviour and fuel consumption.

Component	Fire Behaviour	CBM-CFS3 Pool
Stemwood	The main stem of the tree can either survive or be killed and converted to a snag, depending on severity.	Merchantable
Foliage	Susceptible to combustion at high severity and mortality at all severities.	Foliage
Branches	Smaller diameter classes susceptible to combustion at high severity and mortality at all severities.	Other
Coarse woody debris	Susceptible to combustion at all severities. After fire, uncombusted snags fall down into this pool.	Medium DOM
Forest Floor	Combustion fraction dependent on drought condition; lower susceptibility in F, H, O soil horizons (i.e. Slow pool). After fire at any severity, uncombusted foliage and dead branches transfer to these pools. Uncombusted roots can be transferred into these pools for high severity fires when the main stem experiences mortality.	Above Ground Very Fast (Litter); Above Ground Fast; Above Ground Slow DOM (F,H,O)
Snags	Higher combustion susceptibility at higher severity	Stem, Branch Snag

in Table 1. Though designed for forest GHG reporting, the pool structure of CBM-CFS3 does distinguish between softwood (conifer) and hardwood (broadleaf) that also have large contrasts in both foliage flammability (Alexander, 2010) and ability to survive low to moderate intensity surface fires (Héon et al., 2014). Tree biomass pools are further divided into merchantable tree biomass pools (foliage, stemwood, branches), with separate hardwood and softwood pools for smaller, subcanopy trees. Representative pool values (in t C/ha) per Reconciliation Unit are produced and updated annually based on updated forest inventory and disturbance data. Pool size information by RU is provided in Appendix A. Upon the detection of a forest disturbance such as fire, pool C biomass (both dead and alive) can be transferred to other pools including an atmosphere pool (or remaining the same pool) at proportions prescribed by a Disturbance Matrix. Any live or dead biomass pools combusted immediately are tallied in the direct emissions sums reported here. Live biomass that is killed but not combusted by the fire is tracked, but experiences delayed decomposition on the order of years to decades, and therefore is not tallied within the direct emissions modelling shown below.

2.3 Definitions and assumptions of forest carbon budget after fire

To simplify the process of creating DMs as a distillation of the complexities of fire severity and combustion patterns, the following statements are proposed and maintained throughout:

1. Disturbance matrices are to be in terms of mortality, not survival. Mortality here is defined as tree death by the end of the calendar year of the fire's occurrence. Tree mortality in subsequent years is not modelled here.
2. Crown Fraction Burned (CFB) is a mass-based estimate of the portion of foliage consumed in the flaming passage of a fire, and is inclusive of merchantable and submerchantable trees, both broadleaf and needleleaf. Needles that are heat-killed but otherwise not consumed in the fire are not considered part of CFB, and are instead considered part of the foliage to litter biomass transfer.
3. The heat-killed but unconsumed fraction of the canopy is equal to (mortality minus CFB).
4. In submerchantable trees, mortality is equal to CFB.
5. In merchantable trees, CFB is less than or equal to mortality.
6. Snags are inclusive of both those killed by prior fire as well as those killed by all other causes.

Of these, Crown Fraction Burned (CFB) is an important concept used primarily in fire behaviour science but not carbon accounting nor fire ecology. CFB was introduced in the 1992 Fire Behaviour Prediction System documentation (Group, 1992), and provides a simple continuous 0-100 variable for only the consumption of foliage (inclusive of both conifer and broadleaf). For our purposes, CFB is the desirable metric as opposed to ordinal and less precise systems like Canopy Fire Severity Index (Kasischke et al., 2000) that allows the user to specify which pools of canopy biomass are consumed, but not the precise fraction of each given pool that is consumed.

2.4 Combustion gas emission ratios

Certain variables, like the partitioning of CO₂:CH₄:CO gas emissions, are constant throughout ecozones, but vary by flaming vs smouldering combustion modes. The precise emissions ratios vary slightly between models and field studies, but for this initial algorithm assessment, we define these emissions ratios as being identical to those used in Canada's operational wildfire smoke forecasting system, FireWork (Chen et al., 2019). Emissions ratios are provided in Table 2.

CO₂ is responsible for 86.8% of emissions in the flaming phase, but only 70.3% of emissions in the smouldering phase, with a doubling of CO emissions and tripling of CH₄ emissions (Table 2). With a Global Warming Potential of CO equal to 1.0 and CH₄ of 25, the Global Warming Potential per unit of biomass consumption in the smouldering phase is 1.06 times higher in global warming potential compared to flaming, not including differential aerosol production and injection heights, however. With flaming and smouldering each contributing roughly equally to wildfire emissions, these distinct flaming and smouldering emissions ratios correspond well prior emissions factors used in CBM-CFS3. Note that as currently described, the sum of CO₂,

Table 2. Emissions factors for flaming and smouldering used in this model. Values are the molar fraction of carbon in the unburned biomass and the emitted species, e.g. 87 percent of C in biomass is converted to C as CO₂ in flaming combustion.

Spp	Flaming	Smouldering
CO ₂	0.868	0.703
CO	0.070	0.161
PM ₁₀	0.022	0.048
NMOG	0.016	0.035
PM ₂₅	0.019	0.040
CH ₄	0.005	0.013
BC	0.000	0.000

CH₄, and CO emissions from wildfires only represent approximately 95% of the fire carbon mass emitted to the atmosphere, with 0.5–2.0% of biomass emitted as particulate matter (e.g. PM_{2.5}, but also PM₁ and PM₁₀ classes of particulates at 1 and 10 μm diameters, respectively), and an additional 3% (Hayden et al., 2022) to as little as 1% (Simon et al., 2010) composed of non-methane organic gases that have a large range in global warming potentials as compared to CH₄.

2.5 Ground plot and remotely sensed fire severity data

While remotely sensed fire severity metrics are capable of determining if a specific location falls within a low, moderate, or high severity fire area (Hall et al., 2008a), remotely sensed fire severity metrics alone do not inform estimates of fuel consumption down to specific biomass pools. Instead, this approach uses the change in biomass pools as empirically related to per-pixel satellite spectral reflectance indices (i.e. dNBR, RBR), using detailed and semi-standardized methods of burn severity ground plots with unburned controls (e.g. Cocke et al., 2005; Hall et al., 2008a). Burn severity ground plot measurements are often aggregated into a single “Composite Burn Index” with a weighting scheme originating in southwestern U.S. forests (Key and Benson, 2006; Parks et al., 2019), which are classed into low, moderate, and high severity categories. Plot level measurements of individual forest biomass pools (e.g. conifer overstory mortality or canopy consumption) are recorded as part of the CBI methodology. In this methodology we do not use the CBI aggregated metric itself to infer biomass consumption, but rather compilations of burn severity ground plot measurements that include all the individual biomass pool measurements. Individual burn severity plots were assigned a severity class based on ground observations, and an ecozone-level median biomass pool consumption fraction was computed for each severity class for each biomass pool (see Figure 2). For ecozones without ground plot measurements, an adjacent and ecologically similar ecozone with observations was used.

The field survey data on biomass combustion and mortality rates as stratified by severity class, forms a improved data-driven and ecologically-informed approach to fire direct C emissions estimations here termed FireDMs (Fire Disturbance Matrix-severity).

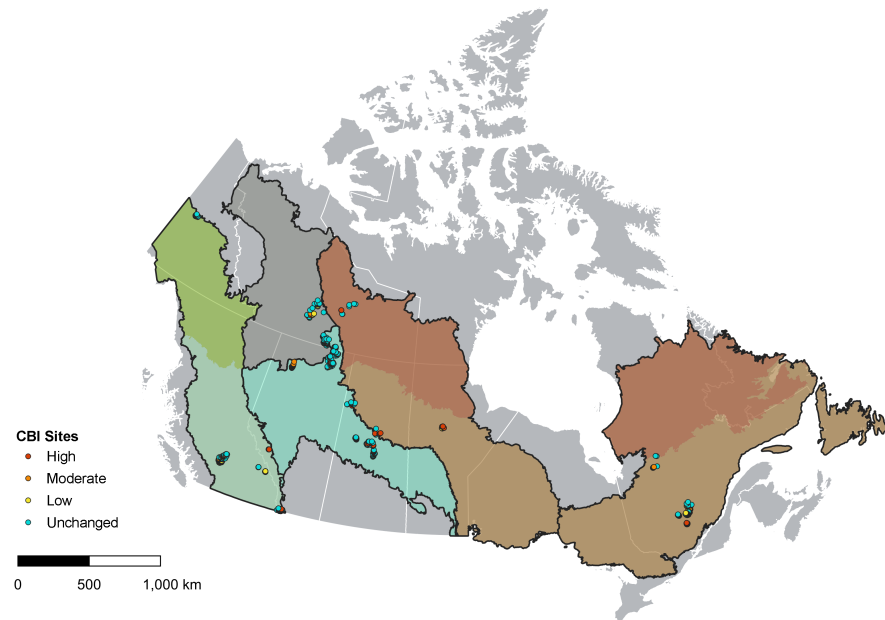


Figure 2. Locations of field-based burn severity plots.

2.5.1 Overstory tree mortality and consumption

Numerous process-driven (Michaletz and Johnson, 2006) or empirical (Hood and Lutes, 2017) tree mortality models are available that show significant skill in predicting tree mortality based on fire behaviour (i.e. flame length, rate of spread). Since the driving data in this model is mapped fire severity over the landscape scale, fire behaviour metrics such as flame length or scorching height of bark are not available as a continuous mapped product. Instead, softwood and hardwood overstory mortality is calculated per ecozone as a function of satellite-observed fire severity using aggregated ground plot data (Table 3).

And since large-diameter, live trees killed by fire do not experience significant live stemwood consumption, the entirety of the live stemwood biomass pool that is killed is transferred to the snag pool. Note that the field data and disturbance modelling undertaken here only accounts for tree mortality within the calendar year of the fire, and delayed mortality of over one year has been documented in boreal low and moderate severity fires (Angers et al., 2011) where less than half of total mortality occurs after the year of the fire. Thus, the modelling here does not account for delayed mortality that may extend upwards of 5 years after fire.

Crown Fraction Burned (CFB) speaks to the fraction of the live canopy that is itself consumed in the flaming front. The alternate outcomes being survival of the foliage, or the mortality of the tree without canopy consumption, resulting in the dropping of foliage onto the forest floor. From the definitions stated earlier, the CFB must be lower than or equal to the

Table 3. Softwood fractional mortality by ecozone, as derived from median values from field studies

Ecozone	Low	Mod	High
BSW	0.45	0.81	1.00
TP	0.45	0.81	1.00
TSW	0.10	0.81	1.00
BP	0.45	0.81	1.00
BC	0.24	0.65	0.98
BSE	0.45	0.81	1.00
TSE	0.10	0.81	1.00
MC	0.28	0.74	0.98
HP	0.45	0.81	1.00
TC	0.24	0.65	0.98
PM	0.13	0.38	0.97
AM	0.28	0.34	0.95
MP	0.28	0.34	0.95
P	0.45	0.81	1.00

mortality rate, using field studies that show any partial crown consumption is likely sufficient to result in high rates if not complete mortality (Hood and Lutes, 2017), which is the case in Canadian trees, which are primarily species with thin bark. Due to the structure of CBM-CFS3, all high severity fires have their mortality in the merchantable and smaller trees set to exactly 1.0, which is no more than a 5% variance from observed values. Ecozone-specific CFB values from field studies of burn severity are summarized in Table 4.

The consumption of live bark biomass is a pool in the model, and consumption rates can be defined by severity class. At the moment, lacking robust field data on bark biomass consumption rates across ecozones and severity classes (which are a small portion of the overall biomass), the bark proportional consumption rate is set to 34% of the overstory mortality rate, based only on a single set well-observed high severity fires in the Taiga Plains by (Santín et al., 2015).

A major distinction is made between softwood and hardwood trees, where in Canada's boreal forests, a large fraction of hardwood trees (see Appendix E) are able to resprout even when the main stem has been killed by an intense forest fire (Brown and DeByle, 1987). Accordingly, the root mortality rates differ greatly between softwoods and hardwoods, with softwood root mortality equal precisely to stem mortality, while in resprouting hardwoods, little root mortality is observed even after intense fire (Pérez-Izquierdo et al., 2019). Though spatially explicit versions of CBM-CFS3 can resolve a species list down to the pixel level, currently an ecozone-level regional average composition of hardwood species with resprouting traits is used and is shown in Table 5.

Table 4. Softwood crown fraction burned by ecozone, as derived from median values from field studies in each ecozone.

Ecozone	Low	Mod	High
BSW	0.0	0.81	1.00
TP	0.0	0.81	1.00
TSW	0.1	0.81	1.00
BP	0.0	0.81	1.00
BC	0.0	0.65	0.98
BSE	0.0	0.81	1.00
TSE	0.1	0.81	1.00
MC	0.0	0.74	1.00
HP	0.0	0.81	1.00
TC	0.0	0.65	1.00
PM	0.0	0.38	0.97
AM	0.0	0.34	0.95
MP	0.0	0.34	0.95
P	0.0	0.81	1.00

Table 5. Ecozone-level average fraction of hardwood overstory species that do not suffer extensive belowground biomass mortality after fire.

Ecozone	Resprout Fraction
BSW	0.75
TP	0.75
TSW	0.94
BP	0.99
BC	0.76
BSE	0.67
TSE	0.78
MC	0.97
HP	0.80
TC	0.27
PM	0.39
AM	0.76
MP	0.32
P	0.99

The fraction of fine roots contained within the combustible forest floor layers (the variable “SW.Prop.Fine.Root.duff” in the model) can be a close to or exceeding 50% of the fine root biomass (Strong and La Roi, 1985); this fine root live biomass is assumed to burn alongside the organic soils (Benscoter et al., 2011). Fine root allocation is between the organic soil (termed “Aboveground” or AG in CBM-CFS3 vs “belowground” or BG for mineral soils) is a parameter that can be RU level and is distinct for hardwoods (HW) vs softwoods (SW). As a result, the calculation for softwood fine root consumption and mortality rate (SW.Mort) are as follows, using softwood as an example:

$$SWFineRootConsump = SW.Prop.Fine.Root.duff \times Duff.Consump.Fract \quad (1)$$

$$SWFineRootMort.AG = SW.Mort \times SW.Prop.Fine.Root.duff \times (1 - Duff.Consump.Fract) \times (1 - ReSproutFactor) \quad (2)$$

$$SWFineRootMort.BG = SW.Mort \times (1 - SW.Prop.Fine.Root.duff) \quad (3)$$

In contrast, the larger diameter of the coarse root biomass pool prevents its consumption during any smouldering of the duff layer, and the mortality rate of coarse roots is simply proportional to that of the stemwood overall.

2.5.2 Understory tree mortality and consumption

Understory (or small diameter overstory) tree mortality is defined separately in the model in the “submerchantable” pool, but given the lack of data on diameter classes in the severity data, robust field data on differing mortality rates of smaller diameter trees is not available, and so the understory tree mortality rate is set equal to the overstory rate as defined in the table above. Note that smaller trees with a top height less than 1.4 m are not considered in this pool, and instead are lumped into the “other” pool.

2.5.3 Litter layer area-wise consumption by severity class

The litter layer forms the first biomass pool in which a spreading fire consumes fuel. In low-severity fires, the litter layer may be consumed little to no underlying duff material consumed, nor any tree mortality (Hessburg et al., 2019). In these low-severity patches, some area of fully unburned forest floor is present, and is summarized from CBI plot data by severity class and ecozone in Table 6. Logically, since litter consumption is largely required for the ignition of the underlying duff layer, this unburned litter areas also informs and constrains duff consumption.

Table 6. Unburned litter area by ecozone and severity class. The majority of the data comes from studies in the Boreal Plains and Boreal Shield West, and so values are extrapolated from those two well-observed ecozones to all others. Ecozones are sorted in order from highest to lowest average annual burned area.

Ecozone	Low	Mod	High
BSW	0.20	0.08	0.05
TP	0.14	0.16	0.03
TSW	0.20	0.08	0.05
BP	0.14	0.06	0.02
BC	0.14	0.06	0.02
BSE	0.20	0.08	0.05
TSE	0.20	0.08	0.05
MC	0.14	0.06	0.02
HP	0.20	0.08	0.05
TC	0.14	0.06	0.02
PM	0.14	0.06	0.02
AM	0.14	0.06	0.02
MP	0.14	0.06	0.02
P	0.14	0.06	0.02

2.5.4 Snag and stump consumption

Dead standing trees and branches on average is a biomass pool much smaller than organic soils or coarse woody debris on the ground, but in local areas of extensive insect killed trees, recent fires, and blowdown, is a substantial biomass pool. Compared to live stemwood of the same diameter, the low moisture content of snags and snag branches allows for much greater consumption during the passage of an intense flaming front (Stocks et al., 2004). The snag branch pool experiences almost complete combustion in high severity fires (Talucci and Krawchuk, 2019), and is highly correlated with live foliage consumption (i.e Crown Fraction Burned) (de Groot et al., 2022). The largest dead wood pool is the standing dead stemwood pool, which remains at most approximately 50% consumed; the consumption of standing snags pool is not quantified precisely in the CBI plot methodology. In the absence of extensive field data from CBI plots to quantify snag consumption, it is estimated as:

$$\text{SnagConsumption fraction} = (0.5 \times \text{CrownFractionBurned}) + 0.05 \quad (4)$$

And for snag branches, field observations (Talucci and Krawchuk, 2019; de Groot et al., 2022) reliably point to a higher rate of consumption for this smaller diameter dead biomass pool:

$$SnagBranchConsumption = (0.9 \times CrownFractionBurned) \quad (5)$$

Stumps are tracked as part of the “Other” pool in CBM-CFS3. As they are typically in contact with the upper forest floor, they are assumed to be consumed at the same rate as coarse woody debris.

2.5.5 Woody debris consumption

Limited data is available on the fraction of woody debris consumption alongside fire severity measurements. Coarse woody debris of overstory stems that makes up 60–80% of woody debris biomass in Canada’s boreal and temperate forests (Hanes et al., 2021), with its moisture and consumption patterns largely follows the moisture regime of the Drought Code (McAlpine, 1995). In this modelling framework, the proportion of coarse (>7.5 cm diameter) and medium (>0.5 cm and <7.5 cm) woody debris consumption is estimated based on detailed measurements of consumption from experimental fires. Coarse woody debris is responsible for approximately 50–75% of the total woody debris load in most ecozones, and approximately 60% of the total woody debris consumption. Ecozone-level CWD consumption rates are summarized in Table 8.

Note that where historical burn severity data from experimental fires is not available, the fire classification type of surface, intermittent crowning, and active crown fire are used instead as proxies for low, moderate, and high severity fire, respectively. Fine woody debris <0.5 cm in diameter is consumed at the exact same rate as the litter pool (see section above).

2.6 Forest Floor Consumption

Unlike canopy consumption metrics that are reliably estimated via burn severity remote sensing, the depth and magnitude of consumption in the forest floor is only weakly related to burn severity metrics, since increasing burn depth in organic soils typically yields little spectral response in remote sensing imagery (French et al., 2020). Furthermore, there is at times a temporal disconnect between consumption in the canopy and the forest floor, with lower-intensity surface fires with a flaming residence time of a minute or less (Wotton et al., 2011) without canopy involvement at times leading to deep smouldering occurring over hours to days afterwards (Huda et al., 2020; Huang and Rein, 2017). Consumption of fine fuels in the litter layer of the forest floor is nearly complete for any given surface fire intensity (Van Wagner, 1972), consumption of deeper organic soil horizons (F+H layers in upland forests and upper peat layers in wetlands) is more dependent on the interaction between moisture content of the soil organic layer and depth of the organic soil (Group, 1992; Davies et al., 2016). While the moisture content of the soil organic layer is not directly observable nor parameterized in Numerical Weather Model (Hanes et al., 2023), it is well-estimated by via simple water balance models within the Canadian Fire Weather Index System (Van Wagner, 1987) the Drought Code and Duff Moisture Code, as well as their composite, the Buildup Index. Given this lack of direct observability of forest floor consumption, this model uses fire weather and fuel loading as inputs to the forest floor consumption model, without consideration of the remotely sensed fire severity observations used in canopy consumption modelling.

In the fire literature in Canada, the soil organic layer is sometimes termed the Forest Floor Fuel Load (FFFL) (Letang and de Groot, 2012) and is dominated by the equivalent organic soil Slow pool (Aboveground Slow Dead Organic Matter, or

AGSlowDOM) in CBM-CFS3. Historically, attention has been paid to the absolute value of Forest Floor Fuel Consumption (*FFFC*) (Group, 1992; de Groot et al., 2009b); however in the case of carbon modelling, it is the relative fraction of consumption (*FFFC/FFFL*) that is of interest. Given the strong empirical evidence that the amount of organic soil present strongly influences the absolute and relative combustion rates (Walker et al., 2020b), modelling of forest floor consumption was conducted on field measurements of the relative fraction of organic soil consumption. In this scheme, we utilize a composite of wildfire data from (de Groot et al., 2009a) alongside the ABoVE duff consumption data (Walker et al., 2020a), with an alternative modelling approach to compute the relative amount of consumption (scalar from 0 to 1) rather than directly modelling an absolute value in kg m⁻² or cm as otherwise done in the literature. A logit transform is used on the scalar data to make it suitable for the fitted non-linear least-squares modelling:

$$\text{logit} \left(\frac{\text{FFFC}}{\text{FFFL}} \right) = [3.91(1 - e^{(-0.008\text{BUI})})] + (-0.53\log_e(\text{AGSlow})) \quad (6)$$

where BUI is the Fire Weather Index System's Buildup Index, and AGSlow in the CBM-CFS3 (given in Mg C/ha in this equation), and also synonymous with the the Forest Floor Fuel Load (with ecozone averages given in (Letang and de Groot, 2012) or site-level data where observed). Assuming an average carbon content of 50%, CBM-CFS3 values in Mg C/ha are converted to fire behaviour units of kg of biomass per squared metre by dividing by 5.

While ultimately this scheme can be used on individual fires with estimated or measured fuel loading and specific BUI values, as an example, an ecozone-averaged fuel load and a multi-year average of BUI during active fire satellite detection can also be used to provide representative values to showcase the modelframework. Specifically, a median BUI of detected fire hotspots in Canada from 2003-2021 (Barber et al., 2024) using the same data as the Canadian CFEEPS-FireWork wildfire air quality model of (Chen et al., 2019) is presented in Table 7, along with proportional consumption values of the forest floor by ecozone.

Note that the maximum upland Forest Floor Fuel Load is approximately 30 kg m⁻² (150 Mg C ha⁻¹) (Letang and de Groot, 2012); higher values are typically seen only in peat ecosystems, where the above scheme is still valid, as approximately 33% of the data used to fit this model is for organic soil pool values over 30 kg m⁻² (>150 Mg Mg C ha⁻¹). Fully 10% of the data used in the FFFC model is for sites with over 60 kg m⁻² of organic soil. Absolute consumption values are similar between deep forest floor organic layers and peatlands (Walker et al., 2020a), though relative consumption rates decline rapidly in deeper organic soil layers, as demonstrated in the model selected here. For Canadian peatlands, the CaMP model (Bona et al., 2020) is instead used in spatially explicit version of CBM-CFS3. Within CaMP, a separate peatland water model driven by Drought Code determines the thickness of the unsaturated peat layer, and an amount approximating 12% of the thickness of the unsaturated peat is consumed as smouldering consumption. The peat-specific carbon pools and fire disturbance matrices are fully described in (Bona et al., 2020); large peatland trees will still utilize the DM scheme described below. Since deeper forest organic soil and peat layers show approximately similar absolute consumption rates, for the purpose of this general model description no peatland-specific components of the fire DMs are required.

Table 7. Fire Weather, fuel loading, and duff consumption values per ecozone. Note that FFFL values are from Letang et al., (2012) and not directly from the Reconciliation Unit values provided in the National GHG Inventory Report. Median Buildup Index of burning is from Barber et al., (2024)

Ecozone	Median Buildup Index of Burning	Median FFFL kg m-2	FFFC kg m-2	% consumption
BSW	58	6.864	2.71	0.39
TP	79	11.97	4.97	0.42
TSW	72	1.7556	1.12	0.64
BP	67	7.1932	3.1	0.43
BC	60	7.67844	2.99	0.39
BSE	40	9.3522	2.55	0.27
TSE	35	4.9764	1.59	0.32
MC	112	4.32	2.88	0.67
HP	52	6.1462	2.33	0.38
TC	59	7.7616	2.98	0.38
PM	60	13.5584	4.34	0.32
AM	39	6.33	1.97	0.31
MP	40	9.3522	2.55	0.27
P	54	7.1932	2.66	0.37

2.7 Calculation of Annual Direct C Emissions from Fire

In an effort to compare model outputs against an independent, large-scale set of fire atmospheric emissions, fire direct atmospheric emissions from the record breaking Canadian 2023 fire season were computed using the above framework. The classified burn severity product from the National Burned Area Composite annual production was utilized (see Hall et al. (2020) for an algorithm description). In NBAC, an internal tracking value “NFIREID” is utilized, which is the final satellite-derived burned area polygon (allowing for multi-part polygons) is split across any RU unit boundaries (if any). Since carbon pool sizes vary across RU boundaries, this allows for a single NFIREID to be present across multiple RUs.

A total of 2199 fires as small as 0.09 ha (one 30x30 Landsat pixel) were mapped in NBAC for burn severity for a total of 14.60 Mha, but only fires over 100 ha were utilized as a lower limit of where meaningful per-fire estimates of the fraction of low, moderate, and high severity burned area was available. Including only fires 100 ha and larger reduced the total number of fires to 966 but the total area remained largely the same at 14.58 Mha. A total of 189,704 ha of post-fire salvage logging was also mapped in 2023 and is assigned to the moderate severity class after consultation with provincial land managers. The direct C emissions from fire shown here are not altered by the act of post-fire salvage logging. Additionally, the NBAC mapping process accounts for unburned islands (and areas with a mapped fire severity no different than unburned) which count towards the total fire area but do not have a disturbance matrix and direct C estimate applied.

Table 8. Coarse Woody debris consumption rates from pre/post measurements in experimental fires

Ecozone	Low	Mod	High
BSW	0.024	0.163	0.140
TP	0.000	0.218	0.238
TSW	0.000	0.218	0.238
BP	0.359	0.509	0.412
BC	0.024	0.163	0.140
BSE	0.080	0.131	0.182
TSE	0.080	0.131	0.182
MC	0.024	0.163	0.140
HP	0.080	0.131	0.182
TC	0.024	0.163	0.140
PM	0.024	0.163	0.140
AM	0.080	0.131	0.182
MP	0.080	0.131	0.182
P	0.359	0.509	0.412

A unique DM was then calculated for each fire using the median area-weighted Buildup Index per fire. All thermal detection hotspots from VIIRS that intersect a fire were extracted from the historical hotspot archive that supports the Canadian smoke emissions model CFFEPPS-FireWork (Chen et al., 2019). The median DC value across all intersecting hotspots was used to derive a single DM per fire, no matter the duration of burning.

To compute total direct fire emissions per fire, a single estimate of the carbon pool size based on the Reconciliation Unit of the centroid of the NFIREID polygon was applied. Fires that cross provincial boundaries are mapped as discrete fires on either side of the boundary in NBAC, but no such division of fires was made across ecozone boundaries. While spatially explicit biomass maps are available for some aboveground components (Guindon et al., 2024) and some organic soil components (Hanes et al., 2022), the majority of the required pool sizes in CBM-CFS3 for the computation of the fire DMs are available only at the spatially referenced RU scale.

3 Results and Discussion

3.1 Direct fire carbon emissions as a function of fire severity and drought

Direct fire emissions per hectare by severity class and as a function of drought condition (Buildup Index) are shown in Figure 3. Direct fire emissions per hectare were greatest (using a constant BUI of 200 as a practical maximum) in the Pacific Maritime ecozone of British Columbia, with 83 and 71 t C/ha released in high and moderate severity fires, respectively. This equates to

295 and 252 t CO₂e/ha and an MCE of 0.90 to 0.89, respectively. The Pacific Maritime ecozone features some of the highest relative contributions of canopy fuels to carbon release, with 32% of modelled emissions from the canopy, and 68% from the surface (i.e. woody debris, litter, duff, roots etc). Next highest emissions were 65 t C/ha from high severity fire in the Boreal Shield East of Labrador which features far lower merchantable volume (see Appendix A) but overall softwood foliage pools only 5% smaller than the Pacific Maritime. Larger aboveground very fast DOM (i.e. litter) pools in the BSE of Labrador offset slightly smaller aboveground slow DOM (i.e. forest floor duff) pools as compared to the PM.

The lowest emissions per area were estimated to be in the Boreal Shield West of Saskatchewan, where total emissions of 16 and 22 t C/ha (56 and 76 t CO₂e/ha) for low and moderate severity fire at a BUI of 200 were 77% in surface fuels. Despite much lower overall emissions, these low emissions fires still feature 77-79% of the total emissions from surface fuels. The Taiga Shield West of the Northwest Territories also was modelled to have emissions of only 21.5 t C/ha under low severity fire.

Across both low and high severity fires, the effect of drought (i.e. Buildup Index) was fairly consistent, the emissions from BUI 200 fires (i.e. very dry conditions) were higher than those of identical severity class but at a much lower BUI of 40. This lower BUI of 40 represents the practical lower limit of large spreading fires in forests in Canada. Eastern regions such as the Mixedwood Plains of Ontario and Quebec as well as the Atlantic Maritime of Nova Scotia and Prince Edward Island see a modelled 60% enhancement of emissions across the range of simulated BUI here, while northwestern boreal regions such as the Taiga Shield West of the Northwest Territories, BSW of Alberta, and Taiga Cordillera of the NWT show a far smaller 10-13% enhancement of emissions per hectare. This patterns is consistent across both high and low severity fire, with the BUI enhancement of emissions as high as 63% in low severity fires, while the effect is only somewhat smaller in high severity fires at 54%. Regions with a high emissions drought sensitivity tend to be those with higher softwood (i.e. broadleaf) forest composition near 50% (by volume) or more (i.e. Atlantic Maritime, Mixedwood Plains and also Boreal Plains of Manitoba). RUs with the highest aboveground slow DOM pools also showed similarly high drought sensitivity of ~42%. RUs with the lowest drought sensitivity tend to also be the RUs with the lowest overall emissions.

3.2 Comparison against existing fuel consumption models

The fire disturbance matrix approach is compared to the FBP System in Figure 4. The FBP used widely in fire growth modelling as well as in Canada's national air quality model (Chen et al., 2019). The FBP fuel consumption values are based solely on experimental (i.e. controlled ignition) fires with fuel consumption measured within less than an hour of the passage of the flaming front, and therefore does not include the consumption from long-smouldering fuel beds such as organic soils and large-diameter woody debris. The FBP system emphasizes the prediction of fire intensity (i.e. flame length) and fire frontal spread rate, with no measurements of the complete fuel consumption. Fuel consumption values provided by the FBP system are dependent only on fuel type (related to leading tree species) and Buildup Index, with no allowance for site-specific variations in fuel load (both canopy and surface fuel loads are fixed in the FBP). Given the need for safe experimental fire operations and the demand for firefighting resources, experimental fires in the FBP with fuel consumption data have a BUI of no more than 80 for the most common C-2 and C-3 fuels. A BUI of 80 exceeds the area-weighted BUI for most years except in the

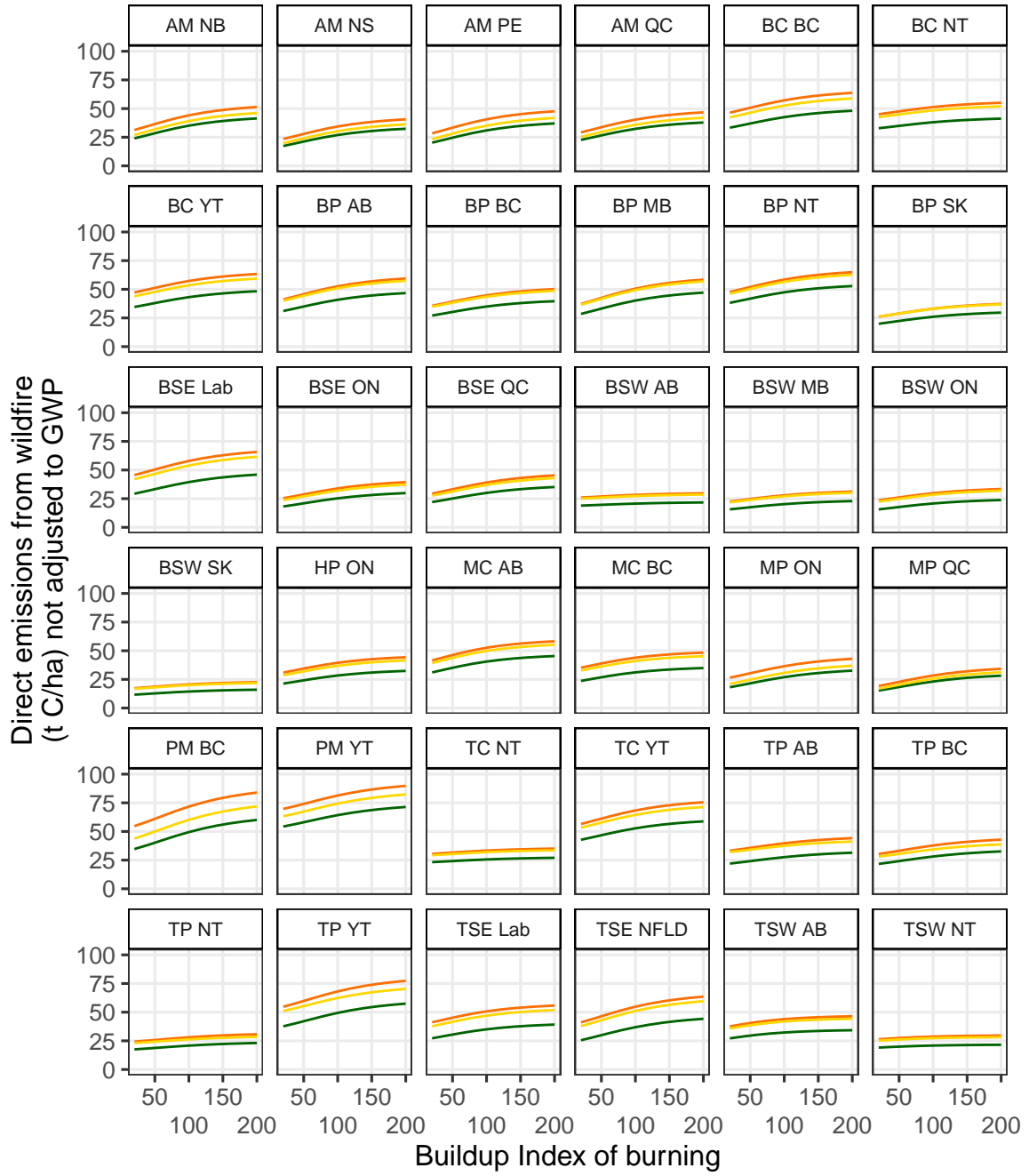


Figure 3. Direct emissions by severity class: orange = high, yellow = moderate, green = low severity. Labelled acronyms are Reconciliation Units (see Figure 1) as Ecozone then Province, so BC is both Boreal Cordillera and British Columbia. Labrador is distinct from the island of Newfoundland for Reconciliation Units, so 'Lab' and 'NFLD' is used. Some small Reconciliation Units without unique NIR biomass pool data are not shown in this figure but are computed still from adjacent RU from the same ecozone. Some RU with very small burned area are also not shown in this figure.

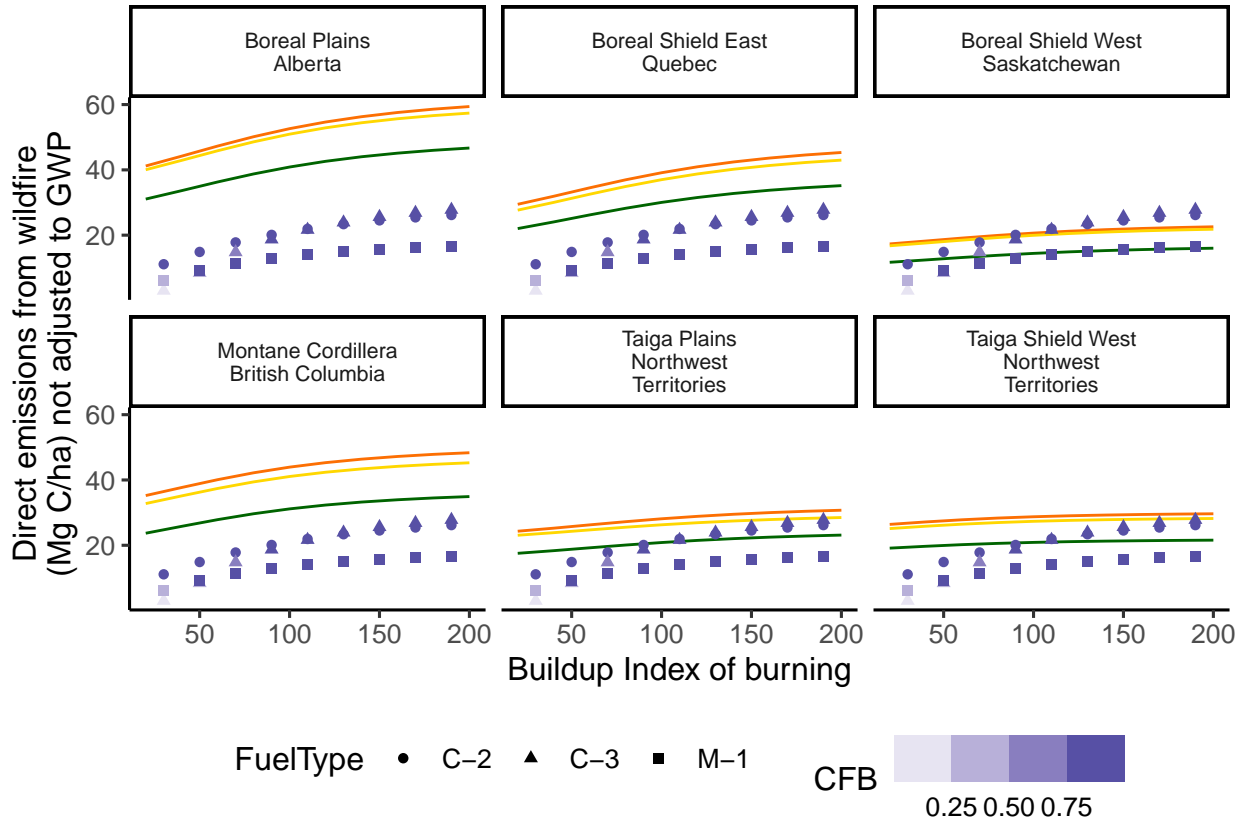


Figure 4. Fire direct emissions by severity class using the FireDMs approach from this study (lines) as compared to Canadian Fire Behaviour Prediction (FBP) System outputs for Total Fuel Consumption, based on experimental fires of differing fuel types C-2 (boreal spruce), C-3 (Jack and lodgepole pine) as well as M-1 (leafless mixedwood 50% conifer). An Initial Spread Index value of 14 is used in all FBP calculations. Points are colourized by Crown Fraction Burned (CFB).

Montane Cordillera ecozone (See Appendix C), though the record-breaking 2023 fire season saw an area-weighted mean BUI for burning days of 109.

The extrapolation of fuel consumption in the FBP beyond 80, coupled with the lack of long-duration smouldering pools, likely accounts for the systematic lower estimates of fuel consumption in the FBP compared to this disturbance matrix approach shown above (see Figure 4). For more southern forests such as the Montane Cordillera, Boreal Plains, or Boreal Shield East, larger canopy fuels and woody debris volumes likely contribute to the larger fuel consumption estimates in this approach compared to the FBP. For the Taiga ecozones, smaller canopy fuel and woody debris fuel loads as well as thin duff layers (i.e. AGSlow in the CBM-CFS3 nomenclature) also contribute to lower total fuel consumption that falls closer to observed FBP Values.

Table 9. Comparison of the Modified Combustion Efficiency (MCE) of airborne gas measurements of Canadian wildfires against modelled MCE

Study	Date	Subset	Ecozone	Buildup Index	Obs MCE	Modelled MCE
Hornbrook et al 2011	2008-07-01	Afternoon (0.2Low 0.4Mod 0.4High)	Boreal Shield West	61	0.92	0.91
Hornbrook et al 2011	2008-07-01	Late Evening (100% low severity)	Boreal Shield West	61	0.82	0.898
Hornbrook et al 2011	2008-07-04	After rain smouldering only low severity	Boreal Shield West	60	0.83	0.898

3.3 Comparison against observed direct fire emissions

3.3.1 Forest fire observations of CO and CO₂ emissions ratios

Mean observed Modified Combustion Efficiency was observed by Hornbrook et al. (2011) for distinct periods during the ARCTAS campaign over northern Saskatchewan in 2008. MCE observed by aircraft during the peak burn period when the majority of fuel consumption and area burned occurs largely corresponded with modelled values (Table 9), suggesting the model provides a fair representation of the balance of flaming and smouldering during large active wildfires. Subsequent smoke plume observations during periods of greatly reduced spread and intensity (late evening and after rain) showed a substantially reduced MCE of 0.82–0.83 that indicates a near lack of flaming combustion. Even when represented as 100% low severity fire in the model, the modelled MCE only declines to 0.903. Since the fire DM model is based on area burned, fire activity such as smouldering but with minimal actual area burned increased is going to show an MCE far lower than areas of low severity fire spread, which are typically still a low sub-canopy flaming front that features a mix of smouldering duff and woody debris alongside flaming consumption of litter (McRae et al., 1994, 2017). During the same ARCTAS campaign over a larger sample of 39 fires, Vay et al. (2011) observed a mean MCE of 0.89 for smoke plumes within 2 km of a large wildfire.

Comprehensive compilations of emissions factors from Binte Shahid et al. (2024) and Andreae (2019) for boreal forest fuels show N₂O emissions factors of 0.205 and 0.24 g/kg, respectively. The N₂O observations from Andreae (2019) are sourced from observations an aggregated MCE of 0.89, similar to our mean modelled MCE of ~0.91. Alternatively, the widely cited emissions factors for N₂O as 0.77% of vegetation N (Lobert et al., 1990; Organization, 1985; Olivier et al., 1994; Davidson and Kanter, 2014) stems from a small number of observations over two Colorado wildfires by Crutzen et al. (1979) that gives a similar result of N₂O:CO₂ ~0.22% by volume, or approximately 0.2 g/kg.

3.4 2023 Canadian wildfire season direct emissions

To calculate the sum total of estimate direct C emission from Canadian wildfires in 2023, severity maps were created for each fire using 2024 season satellite observations using an approach that produces severity class maps using both classified spectral indices (Whitman et al., 2020) with additional fire environment covariates to predict severity class at 30-m !!![cite Ellen's upcoming paper]!!!. A single representative area-weighted Buildup Index value from fire hotspots was computed for each fire. A set of DMs (composed of one DM per severity class) was then applied to Reconciliation Unit carbon stock values for the

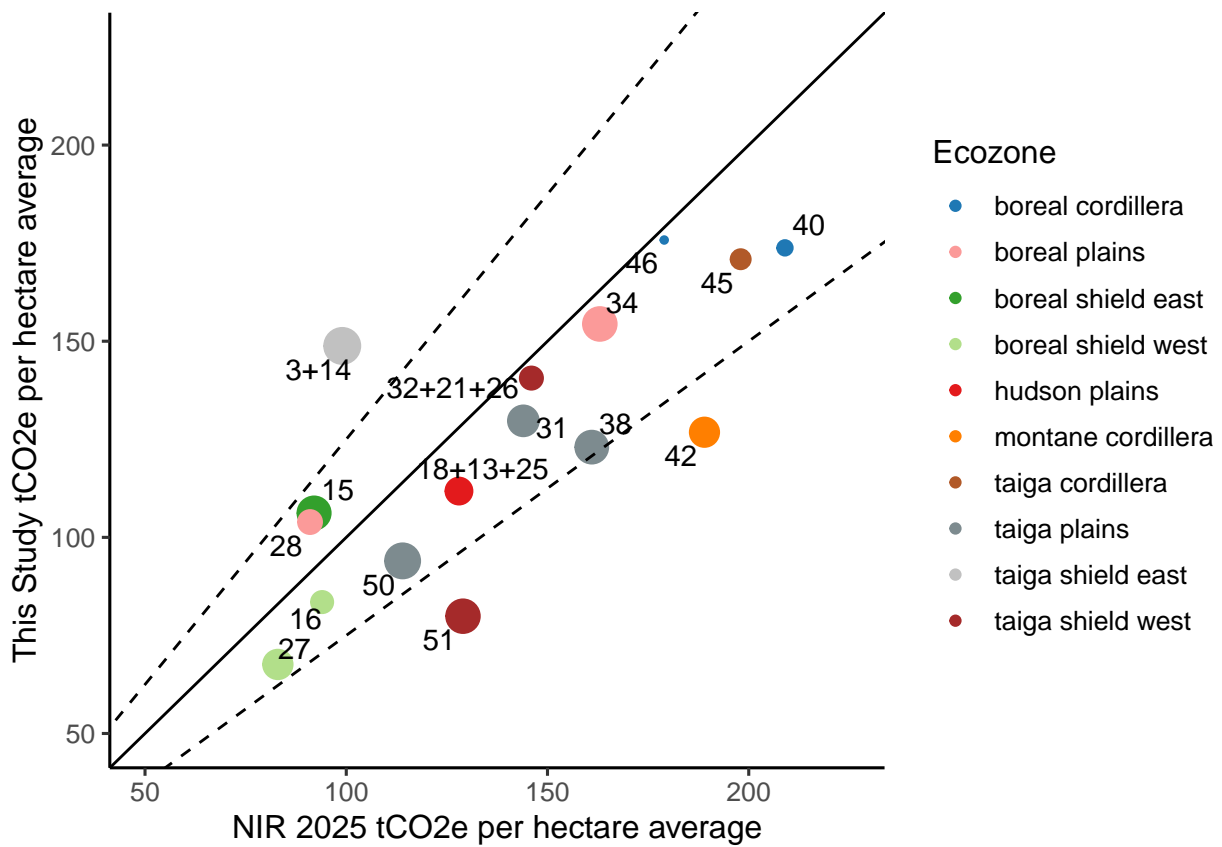


Figure 5. Comparison of CO₂e emissions per hectare between this method at the 2025 National Inventory Report for the 2023 wildfires. Dots are labelled by RU and coloured by ecozone (see Figure 1), with dot size proportional to 2023 area burned. The solid line is the 1:1 reference line, and the dashed line represents 25% deviation from a 1:1 relationship.

total fire area falling into low, moderate, and high severity classes. The same Buildup Index was used for all severity classes per fire event when computing the DM per fire event. Per-fire direct C emissions (i.e. CO₂, CO, CH₄, PM_{2.5}, etc.) were then computed and summed by ecozone and nationally.

RU-level carbon stocks were extracted from the National Forest Carbon Monitoring Accounting and Reporting System (NFCMARS) CBM-CFS3 model results for the start of 2023. Given the extremes of the 2023 fire season, it is reasonable to assume that wildfires occurred indiscriminately across the forested landscape rather than being focused on specific forest types or significantly steered away from fire suppression zones - applying regionally average carbon stocks is correspondingly appropriate.

Table 10. Comparison of per hectare CO₂e direct emissions from this study against the 2025 National Inventory Report for the 2023 wildfire season in Canada. Rows are sorted by decreasing 2023 area burned. Note that for RUs with no managed forest area and no biomass pool data available.

Jurisdiction	Ecozone	Reconciliation Unit	Area Burned (Mha)	Moderate Severity Fraction	High Severity Fraction	Emissions t C/ha	This Study Emissions t CO ₂ e/ha	NIR 2025 Emissions tCO ₂ e/ha
Lab+QC	taiga shield east	3+14	2.50	0.39	0.31	42.3	148.8	99
Northwest Territories	taiga plains	50	2.01	0.23	0.52	26.7	94.0	114
Alberta	boreal plains	34	1.53	0.30	0.42	44.0	154.4	163
Northwest Territories	taiga shield west	51	1.50	0.19	0.58	22.7	79.9	129
Quebec	boreal shield east	15	1.38	0.39	0.27	30.2	106.2	92
British Columbia	taiga plains	38	1.29	0.17	0.65	35.0	123.0	161
Alberta	taiga plains	31	0.88	0.18	0.67	37.0	129.7	144
Saskatchewan	boreal shield west	27	0.70	0.19	0.65	19.2	67.6	83
British Columbia	montane cordillera	42	0.68	0.26	0.39	36.2	126.8	189
ON+QC+MB	hudson plains	18+13+25	0.47	0.23	0.42	31.8	111.8	128
Saskatchewan	boreal plains	28	0.31	0.22	0.41	29.6	103.9	91
AB+MB+SK	taiga shield west	32+21+26	0.28	0.23	0.60	40.1	140.6	146
Ontario	boreal shield west	16	0.25	0.23	0.47	23.8	83.5	94
Yukon Territory	taiga cordillera	45	0.20	0.16	0.49	48.7	170.9	198
British Columbia	boreal cordillera	40	0.14	0.12	0.56	49.5	173.8	209
Yukon Territory	boreal cordillera	46	0.11	0.16	0.58	50.0	175.8	179

Table 11. Comparison of total carbon emissions estimates for the Canadian 2023 fire season. Note that the Byrne et al 2024 estimate shown here uses the emissions ratio for CO inferred from this study. See main text for details.

Source	Approach	TotalEmission
This study	Severity-Inventory	494
Byrne 2024	Total column CO anomaly	510*
CAMS-GFAS	Fire Radiative Power	478
FireWork	Hotspot-FBP	168

A total of 494 Mt C was estimated to be released directly by fires in Canada in 2023. The area-weighted mean Buildup Index for all fires in Canada in 2023 was 109, representing severe but not uniformly exceptional drought conditions in Canada's northern forests. The area-weighted mean total C emissions per unit area was 33.88 t C/ha, though 90% of the emissions per unit area were between the 5th percentile of 14 t C/ha typical of the Taiga Plains ecozone under low drought conditions and the 95th percentile of 54 t C/ha typical of Pacific coastal forests.

Comparison of emissions totals against the NIR is only possible for spatial units (i.e. Reconciliation Units, provinces, or ecozones) where the entire RU is composed of managed forest. In British Columbia, across 2.2 Mha burned, this FireDMs approach estimates were consistently lower than NIR. This was driven by a lower average emissions in FireDMs for both the Taiga Plains with 1.3 Mha burned (124 t CO₂e/ha) and Montane Cordillera with 0.68 Mha burned (127 t CO₂e/ha) as compared to the NIR (161 and 189 t CO₂e/ha, respectively). For Alberta the 1.5 Mha of Boreal Plains ecozone burned showed close agreement (155 vs 163) as well as in the Taiga Plains (130 vs 144). The Taiga Plains fires of both Alberta and British Columbia were largely adjacent, and the FireDMs output was very similar (123 vs 129) across nearly identical moderate and high severity fractions, but the NIR showed a larger contrast (144 vs 161) that may originate from the underlying assumptions of the previous methods of calculating fire emissions in the NIR.

The RU with the largest burned area in 2023 was in the unmanaged forest of Quebec's Taiga Shield East, where NIR pool sizes from the adjacent jurisdiction of Labrador TSE were used in the FireDMs estimates, as no NIR pool sizes were available for Quebec's TSE ecozone area. Over this 2.5 Mha of burned area, the Quebec TSE FireDMs emissions estimates were substantially larger (149 t CO₂e/ha) compared to NIR (99 t CO₂e/ha, see Figure 5). In the Quebec Boreal Shield East ecozone where NIR pools are available, the FireDMs were still larger than NIR, though the gap between the two was much smaller (106 vs 92). Only the Manitoba Boreal Plains and Yukon Taiga Plains showed a similarly larger estimate in the FireDMs compared to NIR, with all other RUs showing a typically 10-30% reduction in emissions in the FireDMs compared to the NIR. Overall, this new emissions estimate method will yield more representative fire emissions estimates that are sensitive to annual differences in drought condition and fire-specific patterns of severity. The small overall impact is likely due to larger soil organic layer emissions in the FireDMs being offset by lower canopy consumption in the low and moderate severity areas.

Byrne et al. (2024) used observed total atmospheric column excess CO and a range of MCE values to estimate total fire C emissions in Canada in 2023 of between 570-727 Mt C with a mean estimate of 647 Mt. The uncertainty in the estimate from

Byrne et al. (2024) lies primarily in the uncertain CO₂:CO ratio (more commonly computed as the normalized ratio MCE) that was estimated to be between 7.8–10.8 g CO₂ / g CO. Our bottom-up estimates that partition flaming vs smouldering shows a lower CO₂:CO estimate of 6. This lower CO₂:CO ratio (i.e. more smouldering) if applied to the data from Byrne et al. (2024) would reduce their lower range of total C emissions to 505 Mt C, which is comparable to the 494 Mt C computed from this bottom-up approach. Estimates of total carbon emissions based solely on the sum of observed Fire Radiative Power (FRP) from Copernicus-CAMS (GFASv1.2 (Kaiser et al., 2012)) was 478 Mt C (Jones et al., 2024). The operational air quality model for Canada produces wildfire smoke emissions estimates using the CFFEPPS-FireWork framework (Chen et al., 2019) which utilizes active fire satellite detections coupled to biomass burning rates from the Canadian Forest Fire Danger Rating System which are known to underestimate total emissions from forest floor combustion (de Groot et al., 2009a). As a result, the CFFEPPS-FireWork total emissions in 2023 with their exceptional nation-wide moisture deficits (Jain et al., 2024) underestimate total emissions compared to other methods, with CFFEPPS estimates of CO emissions only ~40% of satellite observed values (Griffin et al., 2024; Voshtani et al., 2025). Even after assimilating satellite CO and tower-based total carbon measurements, CFFEPPS still retains 20% underestimating bias, likely attributable to an estimate of peak CO (i.e. smouldering) emissions that are lower than reality (Voshtani et al., 2025).

3.4.1 Relationship to other estimates

The forest floor emissions modelling scheme used here builds upon the CanFIRE model (de Groot et al., 2013) which incorporates a similar estimate of absolute forest floor emissions based on fuel type and various Fire Weather Index inputs (including but not limited to Buildup Index). While the CanFIRE model is also capable of estimating tree mortality, the premise of CanFIRE lies in the use of the Canadian Fire Behaviour Prediction (FBP) System to model fire intensity and a physiological-thermodynamic model of tree damage and mortality. CanFIRE is able to run entirely in scenario or forecast mode, i.e. no fire severity map is needed to run the model, unlike the focus here on a mechanism to estimate carbon fluxes and pools after fire severity is mapped. Ultimately, models like CanFIRE can be used for near-real time emissions estimates of direct and indirect fire carbon emissions (and also for prescribed fire planning and scenario testing), while this modelling framework is best used solely operational carbon accounting and reporting given its strong dependence on severity maps. While fire severity can be estimated empirically based on geospatial inputs without observation using multispectral satellite data such as Landsat !!![Ellen's paper]!!!, estimation using coupled fire behaviour and ecology models such as CanFIRE is a more direct approach. Under severe drought conditions and light winds, very large fires often create more wind and energy than is available in gradient winds as measured at nearby airports and fire weather observing stations (Clark et al., 1999). Thus, fire behaviour and fuel consumption models solely driven by wind inputs from distant meteorological stations can under-predict fire intensity and therefore likely fire severity. While fire-atmosphere models are available for research (Coen et al., 2018) and some forecasting and planning purposes (Linn et al., 2020), modelling resources are typically not made available for the extensive and largely unsuppressed fires in northern Canada. Fire severity mapping after the fact is able to account for high fire severity (Whitman et al., 2018) even when fire spread occurs under light winds more associated with lower fire intensity (Whitman et al., 2024).

While the fire DMs presented here are designed for use in NFCMARS for GHG estimation and reporting, their simplicity and similarity to many other forest carbon schema allows them to be used elsewhere such as in other forest dynamics (Brecka et al., 2020) and earth system models (Melton et al., 2020) that require estimates of Canadian forest carbon emissions from wildfire. Stenzel et al. (2019) showed that severity-informed fire C estimates (with snags) in the US are only 30-40% as large as fixed or variable severity data using their LANDIS-type models. Large over-estimates of in-fire bole consumption in models were not observed to correspond to measurements in the field. In the model presented here, our estimates of snag consumption are based on simple but logical relationships with Crown Fraction Burned, but more comprehensive data collection and field observations would be required to extend the accuracy of the snag consumption scheme.

3.4.2 Indirect fire emissions

While fire emissions within the year of the fire are majority of the GHG flux, enhanced post-fire decomposition of dead biomass persists for many years after a fire. The increase in post-fire tree mortality between the year of the fire and the year following the fire is as much as 30% in low and moderate-severity stands (Angers et al., 2011). This extended mortality is not captured in year-of fire severity mapping but is likely better assessed using fire severity data captured the year following fire, as is operation practice in Canada !!!![*cite Ellen's upcoming paper*]!!!. Similarly, the transition of fire-killed stems (snags) from upright to the forest floor woody debris takes between 5-8 years for 50% of stems to fall (Angers et al., 2011) with stemfall rate highest in low-severity fire. Field observations show that initial assessments of fire severity are the primary predictors of snag fall Angers et al. (2011) and decomposition (Boulanger et al., 2011) rates, meaning the mapped severity method used here provides a useful input for multi-year fire carbon modelling of the snag pool in CBM-CFS3. For organic soil pools, fire has been shown to suppress decomposition rates in upland soil pools where drier post-fire conditions are present (Holden et al., 2015), while in permafrost upland (O'donnell et al., 2011) and peatland (Gibson et al., 2018, 2019) systems, fire has profound impacts on soil carbon pools by rapidly increasing thaw depths and subsequent decomposition rates. Currently in CBM-CFS3, decomposition rates are calibrated against field decomposition litterbag experiments (Troyfymow et al., 2002) and annual climate metrics that do not take into account how disturbances such as fire (and fire of varying severity) modify decomposition rates in the absence of a change in climate.

3.4.3 Model gaps

Currently, the model framework only accounts of regionally-averaged soil carbon stocks, meaning that Reconciliation Units with high peatland areas will show higher organic soil slow pool size, but peatlands themselves are not spatially represented in the model, and instead peatlands influence the mean reported Aboveground Slow pool size. Currently, fire disturbance in peatlands is performed by the CaMP model, which uses the closely related Drought Code fire weather metric to estimate peat layer consumption (Bona et al., 2020) and uses the overstory carbon schema of CBM-CFS3 to estimate overstory tree carbon pools and fluxes. Direct satellite monitoring of upland forest organic soil and peatland carbon loss via burn severity monitoring is possible but remains a challenge to implement with accuracy for monitoring purposes (Bourgeau-Chavez et al., 2020). Despite the large carbon stock (c. 500 Mg C/ha from Beilman et al. (2008)), the mean C emissions per area in peatland

due to fire (65 t C/ha) as modelled by Bona et al. (2024) are comparable to regional emissions from peat-rich ecozones such as the Boreal and Taiga Plains under moderate to severe drought conditions. Indeed, it is under these moderate to severe drought conditions under which peatlands burn more frequently (Turetsky et al., 2004; Thompson et al., 2019) and severely (Kuntzemann et al., 2023).

While Canadian wildfires shown an overall selection bias towards preferentially burning older conifer stands (Bernier et al., 2016), fuel selectivity against less flammable portions of the landscape decreases strongly under severe drought conditions (Parks et al., 2018). The severe drought conditions experienced in Canada in 2023 (Jain et al., 2024) are an ideal setting to compare an emissions model using spatially referenced biomass data against observed emissions. The 2023 fires were observed to largely burn boreal forest ecosystems at the same rate as their abundance on the landscape, owing to severe drought and fire weather conditions . Emissions model evaluation against individual fires or in years of less profound drought would be more likely to highlight the limitation of the regionally-averaged carbon pool (i.e. fuel load) values used here. Ultimately, the mapped severity used here is best paired with mapped carbon pools at a similar scale, such as the 1-ha forest carbon modelling for analysis and scenario testing used by Smyth et al. (2024). Future work will extend this fire disturbance algorithm to finer-scale carbon reporting using gridded data as it becomes available for annual reporting purposes.

Species-specific traits in trees with overlapping ranges, such as resprouting in aspen (Brown and DeByle, 1987) but not other broadleaves such as oak or maple, are not explicitly handled in this model. Instead, the relative abundance of trees with contrasting traits that influence ecological outcomes such as fire survival are lumped at the ecozone scale from the aggregation of the plot data. While ecozone-level contrasts in key considerations such as overstory mortality do strongly vary by ecozone (Table 5), the same DM (e.g. hardwood root mortality) is applied in adjacent stands at the same severity class despite the potential for strongly contrasting traits that are readily tied back to mapping at the stand level by leading species. Alternately, models such as CanFIRE can account for species-level contrasts in fire ecology traits, but compiling the relevant ecophysiological properties and traits for all tree species across the spectrum of fire intensity in Canada remains incomplete at this time.

4 Conclusions

Carbon emissions from wildfires in Canada represent a substantial pulse input of greenhouse gases to the atmosphere: the 2023 fire emissions in Canada were an input of approximately 494 Mt C. A modelling framework to extend the current fire and greenhouse gas reporting in Canada is presented. In contrast to the existing modelling system that utilizes a fixed fire severity (i.e. tree mortality) assumption, a field-calibrated satellite fire severity mapping process that follows mature and well-established scientific methods is used. Above-ground carbon pool changes (from live to dead and in situ as well as to the gas phase) rely on a robust field observation dataset that relates back to satellite metrics. Evaluation of the modelling presented above against fully independent airborne observations of CO:CO₂ emissions ratios for boreal wildfires indicates the modelling of proportion of flaming vs smouldering emissions are well-replicated by the model. With confidence in this modelled CO:CO₂

ratio, the total fire CO emissions for the 2023 wildfire season in Canada (with a record 15 Mha burned) is broadly consistent with fire season estimates using satellite total column CO anomalies.

While this prototype carbon flux framework utilizes regionally-averaged carbon stock estimates, future systems deployment within Canada’s carbon accounting system is likely to incorporate precisely mapped (30 m) carbon pools alongside the finely mapped fire severity products (30 m) used here. As both the spatial estimates of carbon stocks across Canada’s forested ecosystems improves alongside additional field observations, it is anticipated that this modelling framework will increase in both accuracy and precision over time.

5 Appendix A: Mean pool size by Reconciliation Unit

Table 12. Carbon pool size (Mg C/ha) for canopy fuels by Reconciliation Unit for 2023. RU are sorted in decreasing size of Softwood Merchantable, the largest average surface pool. Columns are in decreasing mean pool size.

Ecozone	Jurisdiction	RU	Softwood Merchantable	Softwood Other	Hardwood Merchantable	Softwood Stem Snag	Hardwood Other	Softwood Foliage	Hardwood Stem Snag	Softwood Branch Snag	Hardwood Branch Snag	Hardwood Foliage
PM	British Columbia	41	75.7	33.9	3.1	10.1	1.2	9.3	0.4	2.3	0.1	0.1
TP	Yukon Territory	44	33.3	13.0	27.5	5.7	12.1	3.5	4.7	0.8	0.7	1.1
PM	Yukon Territory	47	30.3	17.1	4.1	5.8	2.9	4.7	1.3	1.4	0.3	0.2
HP	Ontario	18	29.8	9.4	3.9	4.8	1.6	4.0	1.0	0.7	0.1	0.3
BC	Yukon Territory	46	26.7	15.7	3.9	6.0	2.5	3.9	1.1	1.7	0.3	0.2
MC	Alberta	36	25.8	19.2	3.1	3.4	2.5	3.8	0.4	1.6	0.2	0.2
BC	British Columbia	40	24.5	22.7	2.8	4.9	2.1	4.6	0.4	2.5	0.2	0.2
MC	British Columbia	42	23.7	13.7	2.8	7.2	1.1	3.6	0.5	1.9	0.1	0.1
BC	Northwest Territories	54	21.1	17.0	1.3	8.4	1.0	3.6	0.7	1.4	0.1	0.1
TC	Yukon Territory	45	20.7	12.2	4.4	6.9	4.1	3.4	2.2	1.4	0.4	0.3
BSW	Ontario	16	20.3	7.7	1.2	4.5	0.5	3.2	0.4	0.8	0.1	0.1
BSE	Newfoundland	1	20.1	16.2	2.7	2.3	2.9	9.3	0.4	1.1	0.2	0.8
TC	Northwest Territories	53	18.6	11.1	0.4	3.8	0.2	2.5	0.1	0.9	0.0	0.0
BSE	Labrador	4	17.8	14.8	0.5	6.2	0.5	8.8	0.2	1.3	0.0	0.1
BP	Alberta	34	16.5	15.1	5.2	3.0	4.8	3.4	1.8	1.6	0.6	0.2
TSE	Labrador	3	16.3	13.4	0.1	9.1	0.2	7.1	0.1	1.2	0.0	0.0
BSE	Quebec	15	15.8	6.9	8.8	2.9	4.4	1.9	1.1	0.6	0.3	0.6
AM	Quebec	11	15.7	7.4	11.0	2.1	5.7	1.3	1.2	0.6	0.4	0.6
AM	Prince Edward Island	6	14.4	6.4	12.6	1.4	7.3	2.7	1.3	0.4	0.4	1.3
BSW	Manitoba	22	14.0	4.9	4.2	4.4	1.4	1.8	1.2	0.6	0.2	0.3
BSE	Ontario	19	13.5	4.9	11.7	1.8	4.9	2.0	1.7	0.3	0.3	0.9
TP	Alberta	31	12.3	11.4	2.5	4.0	2.5	1.9	2.9	1.3	0.4	0.1
AM	New Brunswick	7	12.1	7.6	9.6	1.3	7.6	2.2	1.0	0.5	0.5	0.8
TP	British Columbia	38	11.8	14.9	12.4	1.9	6.8	2.0	2.1	1.0	0.5	0.5
BP	Northwest Territories	52	10.8	20.2	2.1	2.5	7.2	1.8	0.5	2.2	0.8	0.4
BP	Saskatchewan	28	9.2	3.3	10.8	2.9	2.7	1.3	2.6	0.3	0.3	0.4
TP	Northwest Territories	50	9.0	6.3	2.9	2.6	3.4	1.1	0.9	0.5	0.3	0.2
BSW	Saskatchewan	27	8.9	2.9	1.8	5.1	0.6	1.1	1.1	0.5	0.1	0.1
AM	Nova Scotia	5	8.8	2.9	17.6	1.1	7.4	1.0	1.9	0.2	0.4	1.2
BP	Manitoba	23	8.1	3.4	12.0	2.2	4.2	1.4	3.3	0.4	0.4	1.5
BP	British Columbia	39	7.3	8.7	19.7	2.1	9.2	1.8	2.9	1.0	0.8	0.7
TSW	Alberta	32	6.5	11.5	2.2	3.0	5.0	2.6	1.5	1.3	0.5	0.2
TSW	Northwest Territories	51	4.6	10.5	0.7	2.1	1.3	1.7	0.4	1.7	0.1	0.1
BSW	Alberta	33	1.1	6.2	1.2	1.0	7.0	1.5	1.4	1.2	1.6	0.3

Table 13. Carbon pool (Mg C/ha) for sub-canopy fuels by Reconciliation Unit for 2023. RU are sorted in decreasing size of Aboveground Slow DOM, the largest average surface pool. Columns are in decreasing mean pool size.

Ecozone	Jurisdiction	RU	Aboveground Slow DOM	Medium DOM	Aboveground Fast DOM	Aboveground Very Fast DOM	Softwood Coarse Roots	Hardwood Coarse Roots	Belowground Fast DOM	Belowground Very Fast DOM	Softwood Fine Roots	Hardwood Fine Roots
PM	British Columbia	41	58.3	19.1	16.1	8.7	24.1	0.8	3.0	1.4	2.3	0.1
PM	Yukon Territory	47	46.1	32.2	22.8	25.5	10.1	3.5	3.6	4.1	1.4	0.5
TP	Yukon Territory	44	46.0	22.3	14.7	15.4	9.9	9.5	3.2	2.5	1.1	1.0
BSE	Newfoundland	1	44.2	5.9	9.3	10.2	8.7	2.7	1.5	1.3	1.4	0.4
TC	Yukon Territory	45	42.0	29.2	19.9	14.7	7.0	3.5	3.5	2.9	1.0	0.6
BSE	Labrador	4	41.5	13.0	11.2	11.4	7.7	0.2	1.6	1.7	1.5	0.0
BP	Manitoba	23	39.5	12.7	5.4	12.0	2.3	5.1	1.4	1.5	0.5	1.0
AM	New Brunswick	7	38.8	7.0	9.8	6.9	4.1	5.4	1.8	1.1	0.7	0.9
BP	Northwest Territories	52	38.5	7.4	20.8	9.9	6.2	3.8	2.2	2.3	1.1	0.7
BP	Alberta	34	37.8	10.4	14.8	6.6	6.7	3.2	2.4	1.6	1.0	0.6
BC	British Columbia	40	37.6	9.6	18.0	9.8	10.0	1.0	2.2	2.1	1.5	0.2
MC	Alberta	36	35.6	12.2	15.7	7.7	9.4	2.6	2.4	1.8	1.4	0.4
AM	Prince Edward Island	6	35.4	6.1	5.8	7.4	4.4	5.0	1.1	1.0	0.8	0.9
BC	Yukon Territory	46	34.8	21.2	16.1	11.8	9.0	2.9	2.8	2.6	1.3	0.4
AM	Quebec	11	33.8	9.0	8.7	7.1	4.6	5.0	1.8	1.3	0.8	0.9
BSE	Quebec	15	32.0	10.7	8.1	8.4	4.6	4.1	1.7	1.5	0.9	0.7
AM	Nova Scotia	5	31.4	6.0	4.9	6.1	2.2	6.3	1.1	0.9	0.6	1.2
TSE	Labrador	3	30.7	15.2	10.3	8.0	6.7	0.1	1.9	1.8	1.5	0.0
BP	British Columbia	39	29.3	10.1	10.9	7.8	3.3	5.9	1.6	1.4	0.7	0.8
MC	British Columbia	42	27.8	12.9	11.5	5.3	7.9	0.8	2.3	1.2	1.2	0.1
BSE	Ontario	19	27.3	8.1	5.7	7.9	3.8	5.0	1.2	1.3	0.7	0.9
HP	Ontario	18	26.3	14.6	6.5	7.8	8.2	2.5	1.4	1.8	1.4	0.5
TP	British Columbia	38	25.7	7.6	10.1	7.8	5.4	3.9	1.4	1.6	1.0	0.5
TP	Alberta	31	24.2	21.9	11.2	5.4	4.8	1.9	2.6	1.7	0.9	0.5
BC	Northwest Territories	54	23.7	31.7	15.8	10.3	7.8	1.6	2.4	2.7	1.5	0.3
TSW	Alberta	32	22.2	19.2	12.7	6.3	3.8	3.0	2.4	1.8	0.8	0.7
BP	Saskatchewan	28	21.4	13.3	5.0	6.0	2.5	4.1	1.5	1.4	0.6	0.8
BSW	Ontario	16	20.0	10.7	6.0	5.2	5.7	0.5	1.3	1.3	1.3	0.1
BSW	Manitoba	22	17.2	14.8	4.7	6.1	3.7	2.3	1.3	1.6	0.9	0.5
TP	Northwest Territories	50	13.9	13.1	6.9	8.1	2.9	2.7	1.5	2.4	0.8	0.7
TC	Northwest Territories	53	11.3	24.1	9.4	10.0	5.7	0.5	1.4	3.0	1.5	0.1
BSW	Alberta	33	11.0	11.5	11.6	5.0	1.6	3.3	2.2	1.4	0.4	1.0
BSW	Saskatchewan	27	10.9	13.0	3.7	4.2	2.2	1.2	1.4	1.2	0.6	0.3
TSW	Northwest Territories	51	10.4	11.9	10.1	5.8	3.0	1.2	1.9	2.1	0.7	0.3

6 Appendix B: Non-linear least squares modelling of soil organic layer consumption

For national annual estimates of forest organic soil layer consumption during wildfire, implementations that only utilize Canadian experimental fire data from the Fire Behaviour Prediction System will be limited to a maximum consumption value of 5 kg (biomass) m⁻² of total surface fuel (woody debris, litter, and duff) of 5 kg m⁻², or 25 Mg C ha⁻¹, given the observation dataset and fitted model parameters. For the common “C-2” boreal spruce fuel type for instance, Surface Fuel Consumption, SFC (biomass units in kg m⁻² not kg C) is modelled as:

$$SFC = 5.0 \left(1 - e^{-0.0115 BUI}\right)^{1.0} \quad (7)$$

This model form has the distinct advantage of SFC being 0.0 at a BUI of zero. The model parameters vary by fuel type (i.e. deciduous broadleaf fuels are limited to 1.5 kg m⁻² of maximum SFC) but are fixed within a fuel type.

More recent observations and modelling from de Groot et al. (2009a) extended the FBP data with an additional 128 observations from 7 additional wildfires, and the ABoVE project compiled over 1,000 field observations of depth of burn and C stocks before and after wildfire in Canada and Alaska, over 600 of which are in North American Level II ecoregions also occurring in Canada (Walker et al., 2020a). de Groot et al. (2009a) provides a concise and informative improvement on the FBP fuel consumption equations, where both a Fire Weather Index System component (in this case, Buildup Index) is used similarly to Buildup Index in the FBP, but importantly, the site-level organic soil layer fuel load is also accounted for, which allows for the greater absolute combustion in deeper organic soils that is moderated by the natural logarithm transformation:

$$\log_e(FFFC) = -4.252 + 0.710\log_e(DC) + 0.671\log_e(FFFL) \quad (8)$$

where FFFC is Forest Floor Fuel Consumption (SFC minus surface woody debris) in kg (biomass) m⁻² and FFFL is Forest Floor Fuel Load in kg m⁻². The forest floor as defined here is inclusive of the litter and duff layers, live mosses and lichens. This model presented above fits well within the dataset and extends the observed maximum FFFC to nearly 10 kg m⁻². The ABoVE synthesis of FFFL and FFFC (Walker et al., 2020a) expands upon a slightly smaller dataset used in a modelling summary also by Walker et al. (2020b), where structural equation modelling was used to explore drivers of FFFC but no concise and readily reproducible modelling is produced. The results of the SEM from Walker et al. (2020b) emphasized a greater role of FFFL over DC, though coarse reanalysis that lacked local fire agency weather stations was used. An analysis of just 2014 fires in the Northwest Territories by Walker et al. (2018a) showed that while the mean depth of burn across all black spruce stands was 6-10 cm, the driest (xeric) black spruce stands with the smallest FFFL showed upwards of 75% soil organic consumption, while deeper organic soils in subhygric black spruce stands showed less than 25% consumption.

To provide the largest possible dataset for FFFC and FFFL, the ABoVE synthesis was combined with wildfire data from de Groot et al. 2009 not otherwise found in the ABoVE synthesis. The ABoVE synthesis sites in the Alaska Boreal Interior ecoregion, which have equivalent Canadian ecozone were excluded due to the presence of continuous permafrost and deep organic soils, but Alaska Boreal Cordillera sites near the Yukon border were utilized. Experimental fire data from the FBP

data was not used, as deeper combustion measurements resulting from hours and days of smouldering combustion captured in wildfire data are not available in experimental fires where extensive smouldering is not measured due to suppression.

For the purposes of improving national estimates of the fractional soil organic layer loss during wildfire, this framework emphasizes the proportional C stock loss (as with all CBM-CFS3 disturbance matrices) rather than the absolute value of combustion. In contrast to the modelling of absolute combustion value, any analysis of proportions is best conducted as logit-transformed data, where the logit transformation is:

$$\text{logit}(p) = \log \frac{p}{1-p} \quad (9)$$

which effectively transforms a data of proportions of [0,1] to a Gaussian distribution with a range of approximately -5 to +5 (in this dataset), and a mode approximately at zero.

In the logit transformed space, saturation-type non-linear curve using the relevant FWI component was fitted in a non-linear least squares model, but an additive term of the natural-logarithm transformed forest floor fuel load (FFFL) (given as AGSlow pool in Mg C/ha) was used as well. The non-linear least squares model fit was conducted using the Levenberg-Marquardt nonlinear least-squares algorithm found in MINPACK (Elzhov et al., 2023) R package, which supported bounded parameter constraints.

In the abstract, the model follows the form:

$$\text{logit} \left(\frac{\text{depthofburn}}{\text{pre-fireorganicdepth}} \right) = [c(1 - e^{(a\text{BUI})})] + (b \log_e(\text{AGSlow})) \quad (10)$$

with fitted parameters as:

$$\text{logit} \left(\frac{\text{depthofburn}}{\text{pre-fireorganicdepth}} \right) = [3.50(1 - e^{(-0.008\text{BUI})})] + (-0.53 \log_e(\text{AGSlow})) \quad (11)$$

Note the “b coefficient on the parameter associated with the forest floor fuel load (AGSlow) of -0.53, which results in larger organic layer fuel loads leading to smaller proportional consumption values, which follows the patterns shown by Walker et al. (2018b) for NWT fires of 2014.

The a parameter term that forms the exponent of e alongside the Buildup Index is related to the BUI value at which half of the maximum possible asymptotic consumption value is observed (for a given FFFL value). The NLS fitting was given a minimum value of -0.008 such that a 50% consumption rate was modelled as occurring at or around a BUI value of 70 for typical upland spruce forest floor (FFFL of 8 kg/m² or AGSlow of 40 t C/ha) following the wildfire data of de Groot et al. (2009b) as well as experimental fire observations in spruce forests from the FBP System. The other parameters were fit to the best possible value with no constraint.

For example, using a moderately thick ~12 cm thick organic soil layer, the proportion of consumption as a function of Buildup Index using the model above:

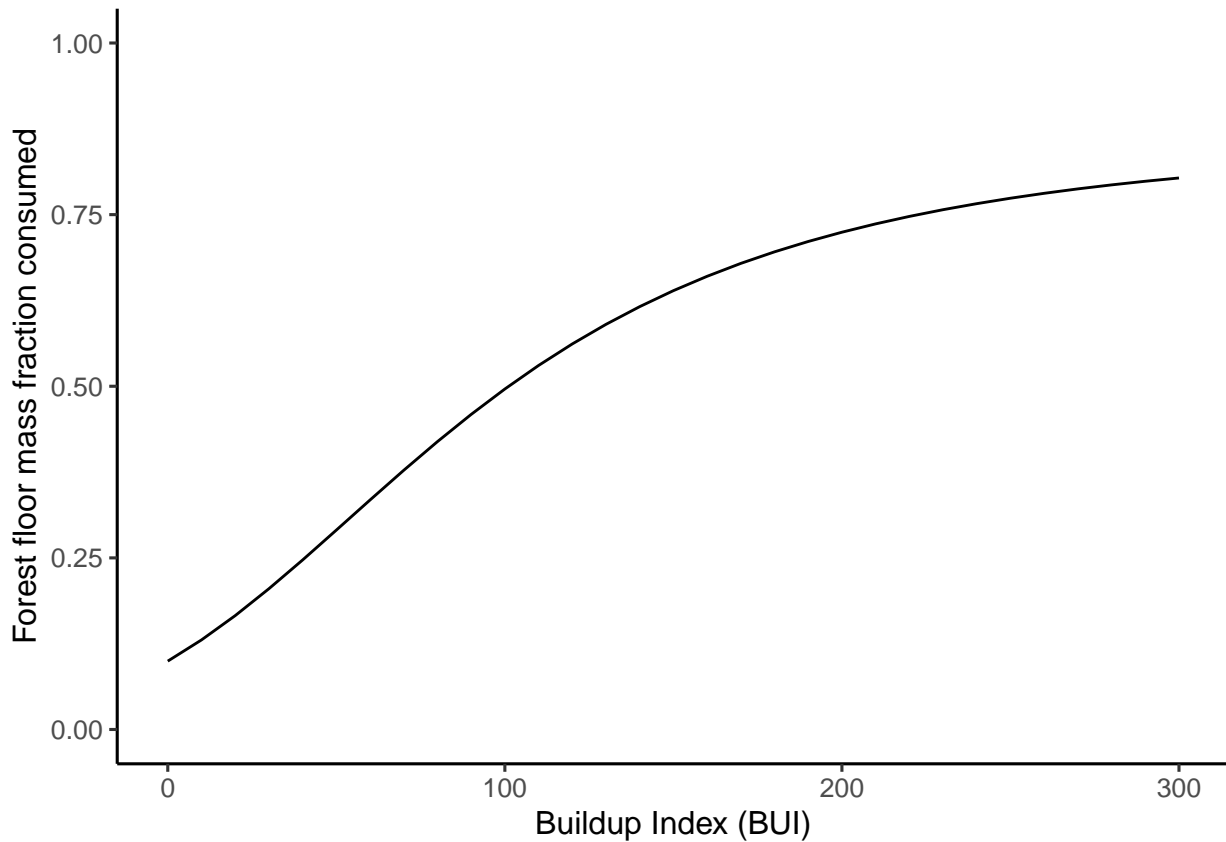


Figure 6. Example of the forest floor consumption model for a duff layer (AGSlow) of 60 Mg C ha⁻¹ (12 kg m⁻²)

With the parameter constrained NLS fitting, the proportional consumption model for the forest floor has a leave-one-out (conducted at the fire-level, not plot) cross validated r^2 of 0.52 and a Mean Percent Error of 45%

Across the entire parameter space of Buildup Index and AGSlow pool size, the following isolines of proportional consumption in the model can be plotted:

7 Appendix C: Annual variability in observed Buildup Index during wildfire spread, and impact on modelled ecozone-level forest floor emissions

8 Appendix D: Representative photos

9 Appendix E: List of Resprouting Hardwoods of Canada

Alnus spp. Arbutus men. Betula all. Betula pap. Betula pop. Fraxinus ame. Fraxinus nig. Fraxinus pen. Populus bal. Populus gra. Populus tre. Populus tri. Quercus spp. Salix spp.

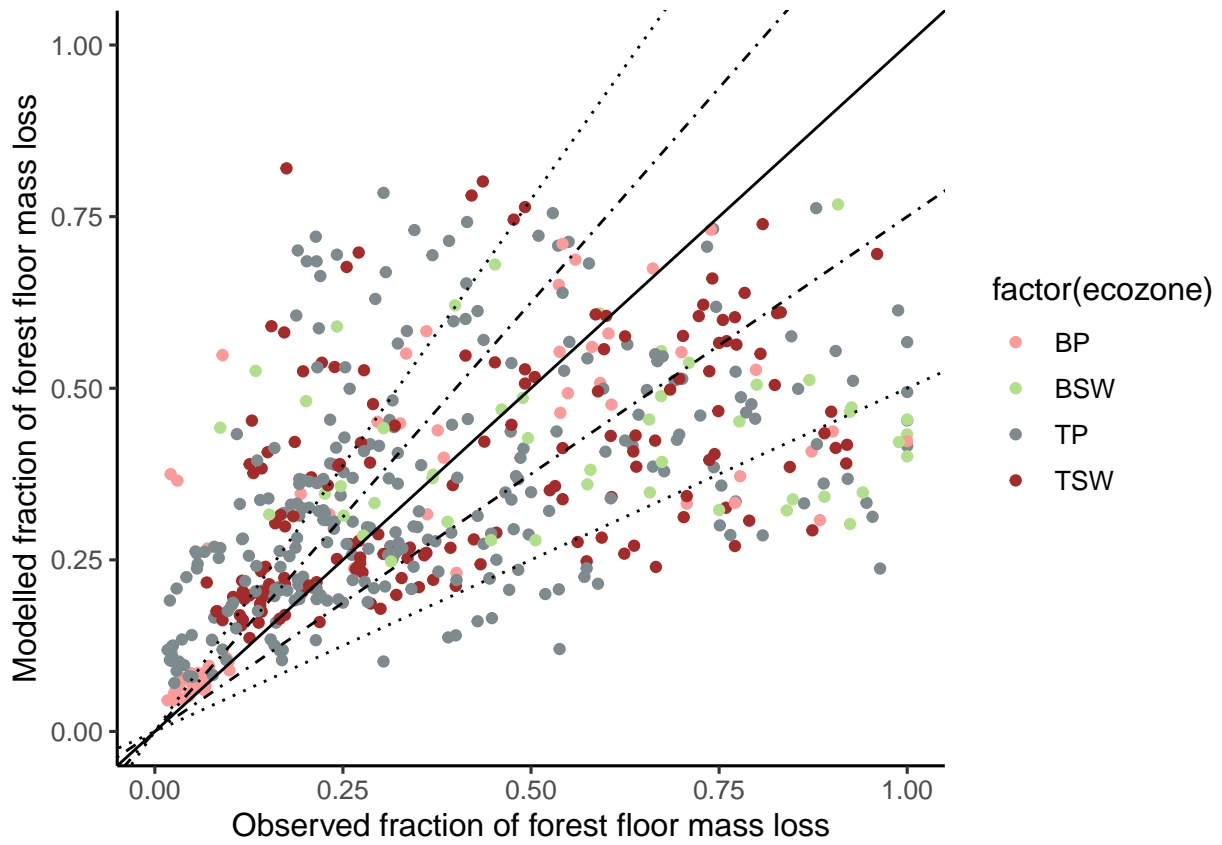


Figure 7. Leave one out cross-validation of the forest floor consumption model. Where multiple measurements were conducted within a single fire, the entire fire was excluded from the training data used in the model training.

10 Appendix F: Disturbance Matrix Examples

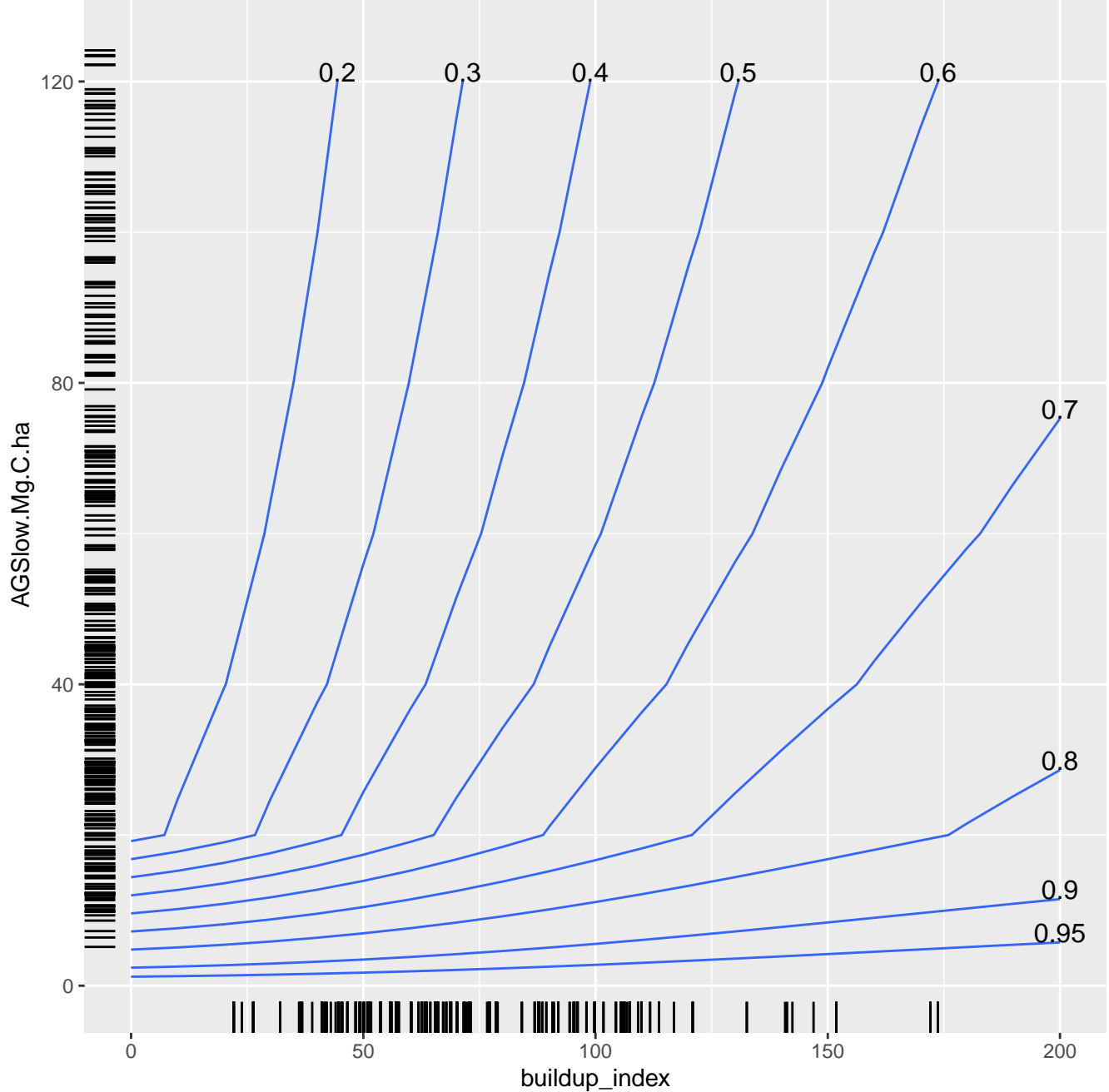


Figure 8. Isoline contours of equal organic soil layer consumption fraction as a function of BUI and the organic soil layer (Medium DOM) Carbon pool in Mg C/ha. Field observations of burn from 547 field measurements across Canada from the Yukon-Alaska border to Manitoba. Rug plots at the axis margins show the marginal density of the data.

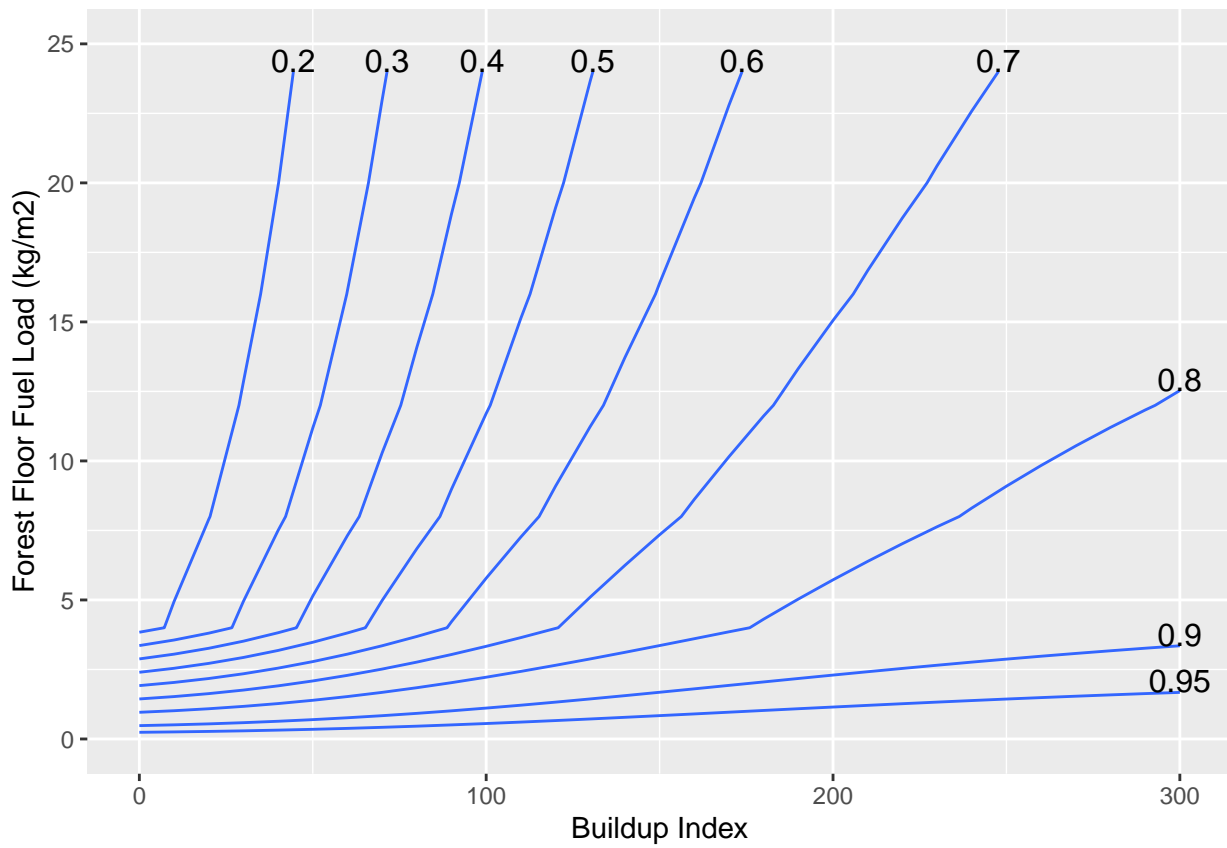


Figure 9. Isoline contours of equal organic soil layer consumption fraction as a function of BUI and the organic soil layer (Medium DOM) Carbon pool in Mg C/ha. Field observations of burn from 547 field measurements across Canada from the Yukon-Alaska border to Manitoba.

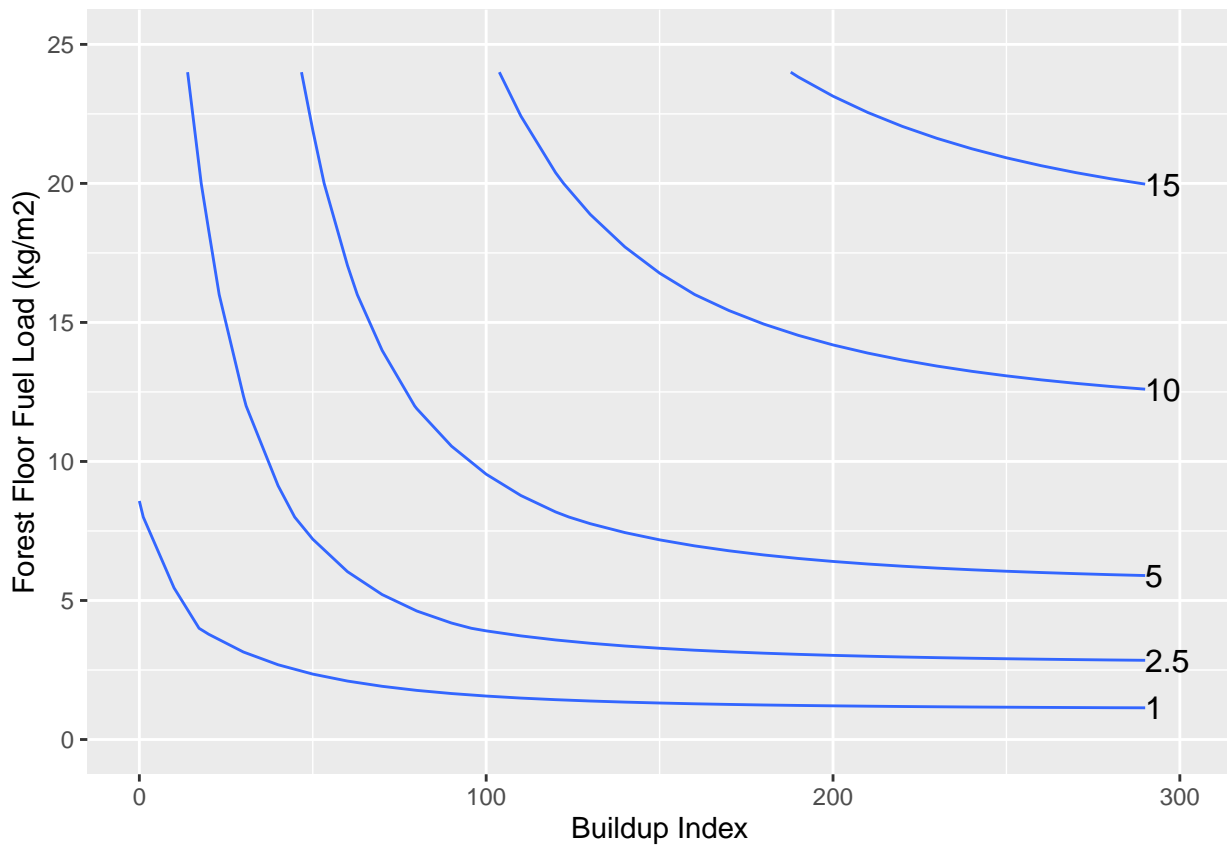


Figure 10. Isoline contours of equal organic soil layer consumption in kg/m² as a function of BUI and the organic soil layer fuel load in kg/m². Field observations of burn from 547 field measurements across Canada from the Yukon-Alaska border to Manitoba. Note that peatland ecosystems begin at approximately 50 kg/m² of forest floor fuel load, or approximately 40 cm organic soil thickness.

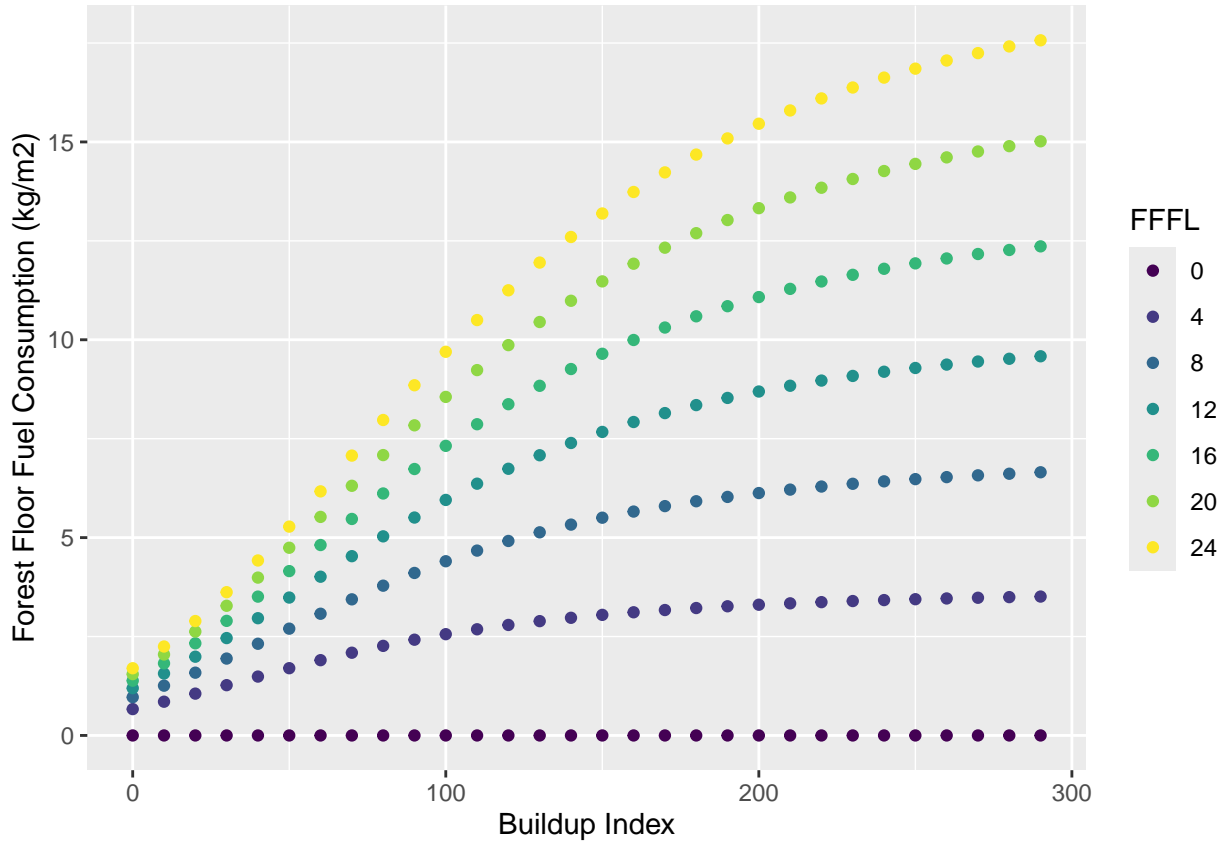


Figure 11. Forest floor consumption as a function of BUI across varying levels of forest floor fuel load (FFFL), as shown by coloured dots.

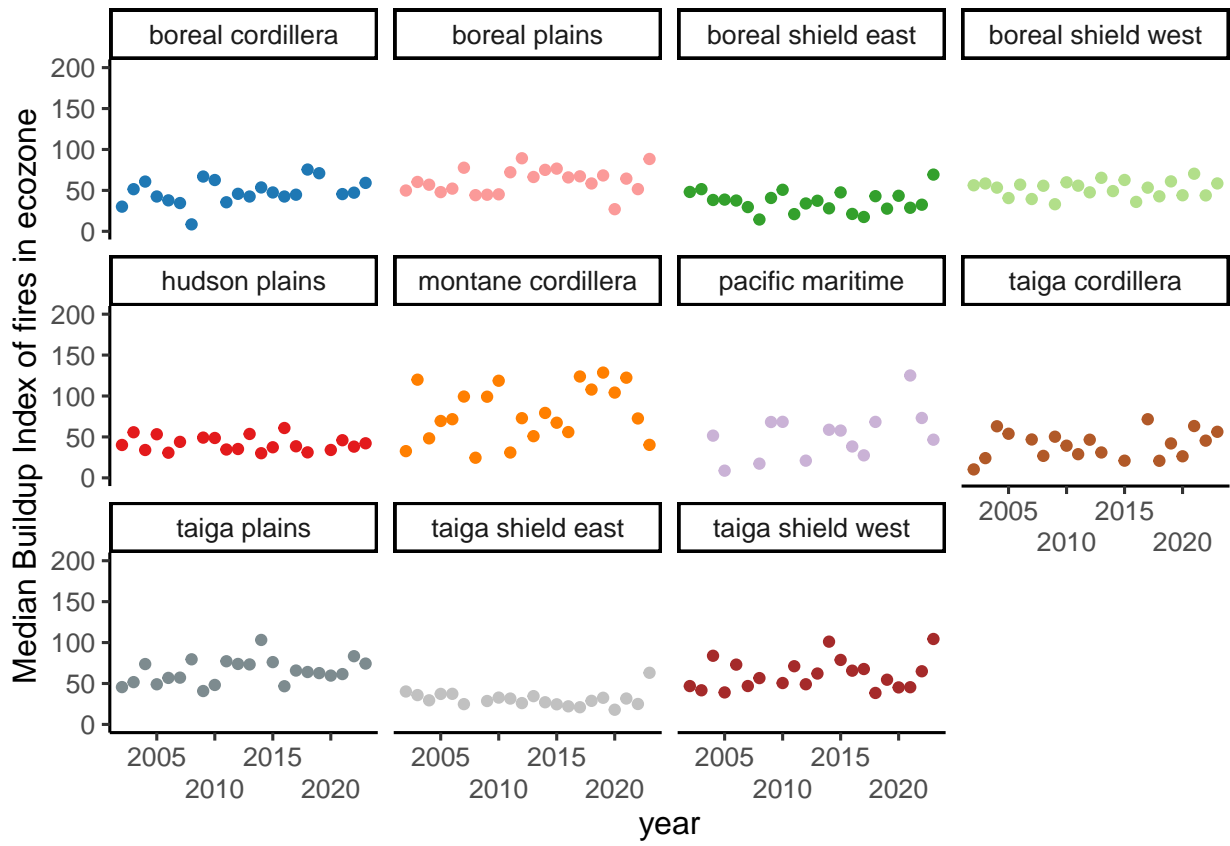


Figure 12. Annual variability in area-weighted median BUI of active fire spread days by ecozone.

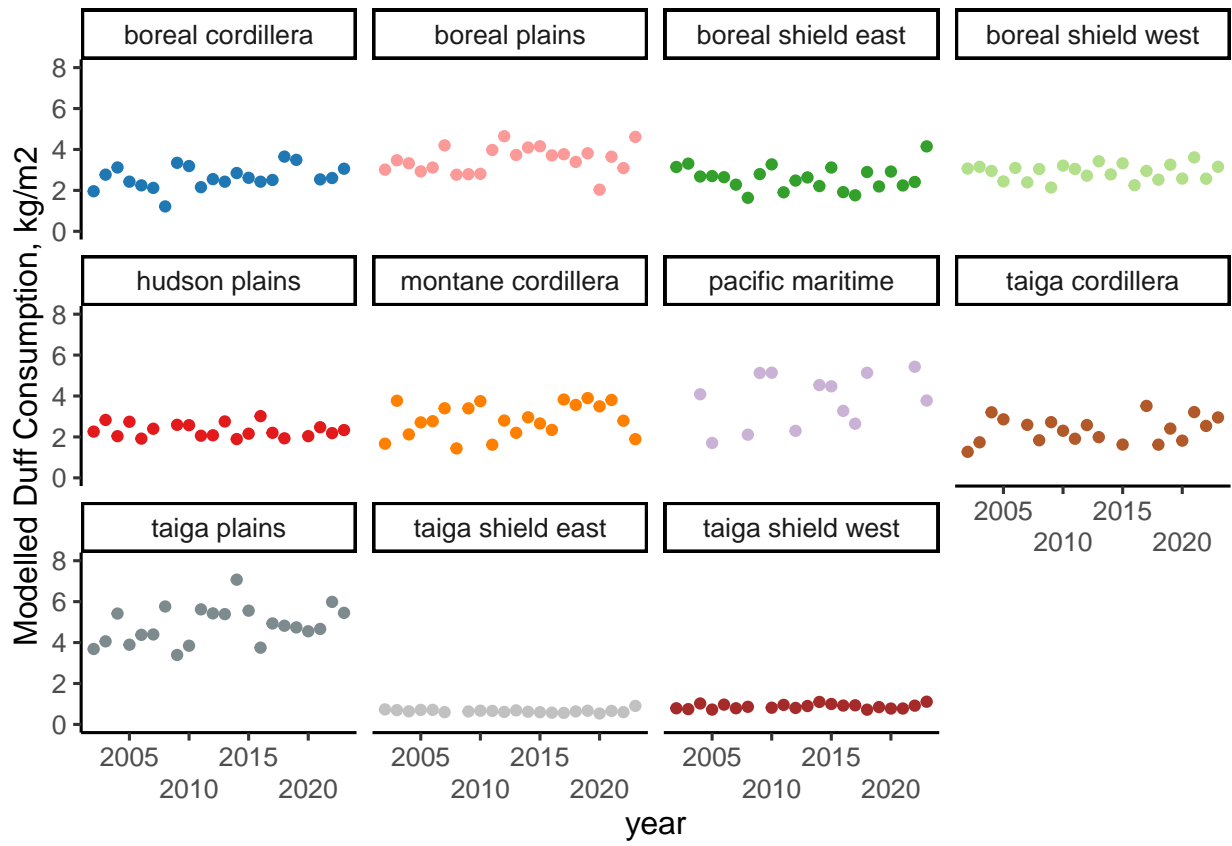


Figure 13. Annual variability in forest floor median consumption values by ecozone.

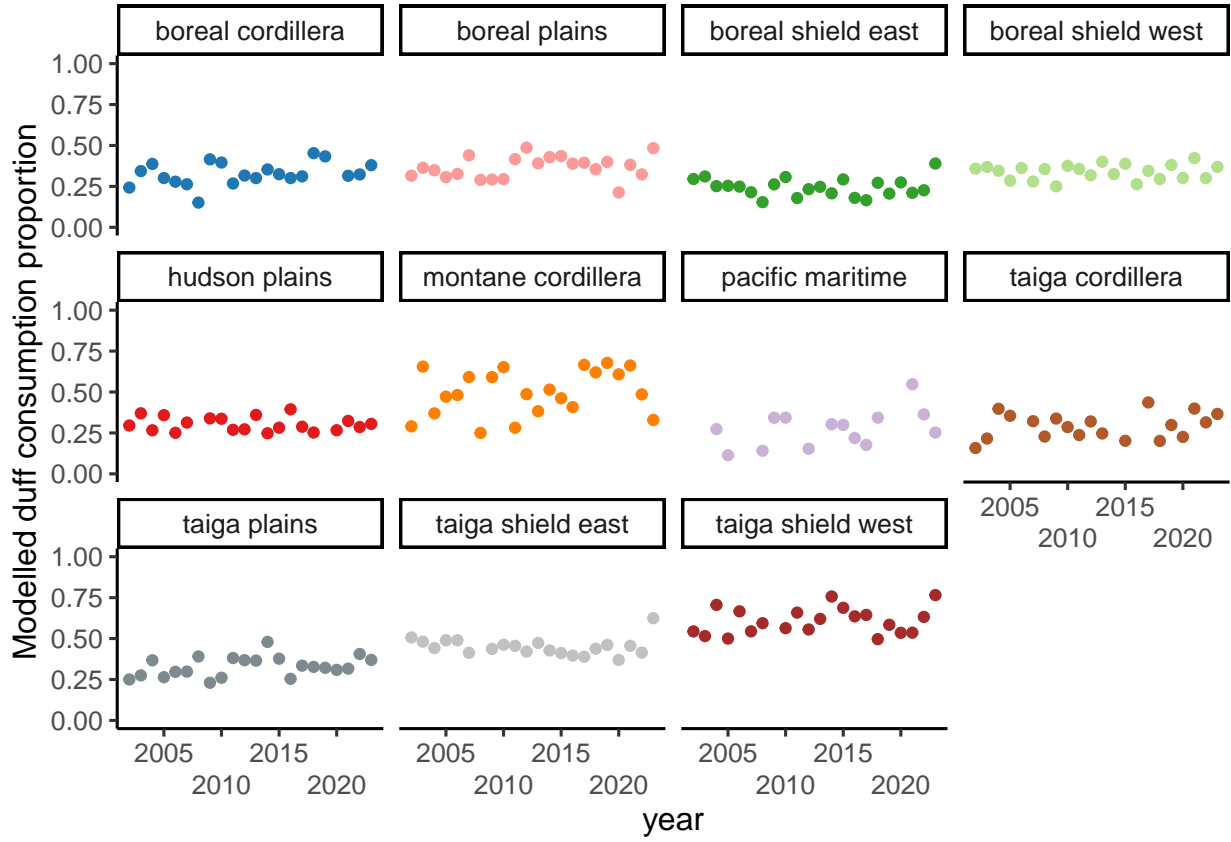


Figure 14. Annual variability in forest floor proportional consumption by ecozone.



Partial area-wise burning of thin litter and duff layer in a boreal pine-aspen mixedwood stand following surface fire, one year after fire. Note low consumption of woody debris and snags.

Figure 15. Appendix D: Examples of fire ecology processes captured in FireDMs from field-based burn severity plots.



Partial area-wise burning of thin litter and duff layer in a boreal pine-aspen mixedwood stand following surface fire, one year after fire. Note low consumption of woody debris and snags.

Figure 16. Appendix D: Examples of fire ecology processes captured in FireDMs from field-based burn severity plots.

Table 14. Low severity Disturbance Matrix in BP. Note: only some biomass and atmospheric pools are shown.

	Softwood Merchantable	Softwood Stem Snag	Medium DOM	Softwood Foliage	Aboveground Very Fast DOM	CO2	CH4	CO	PM25
Softwood Merchantable	1	0.000							
Softwood Stem Snag		0.475	0.475			0.043	0.000	0.004	0.001
Medium DOM			0.551			0.315	0.006	0.072	0.018
Softwood Foliage				0.55	0.45	0.000	0.000	0.000	0.000
Aboveground Very Fast DOM					0.14	0.746	0.004	0.060	0.016
CO2									
CH4									
CO									
PM25									

Table 15. Mod severity Disturbance Matrix in BP. Note: only some biomass and atmospheric pools are shown.

	Softwood Merchantable	Softwood Stem Snag	Medium DOM	Softwood Foliage	Aboveground Very Fast DOM	CO2	CH4	CO	PM25
Softwood Merchantable	0.19	0.81							
Softwood Stem Snag		0.00	0.545			0.395	0.002	0.032	0.009
Medium DOM			0.462			0.379	0.007	0.087	0.022
Softwood Foliage				0.19	0.00	0.703	0.004	0.057	0.015
Aboveground Very Fast DOM					0.06	0.816	0.005	0.066	0.018
CO2									
CH4									
CO									
PM25									

Table 16. High severity Disturbance Matrix in BP. Note: only some biomass and atmospheric pools are shown.

	Softwood Merchantable	Softwood Stem Snag	Medium DOM	Softwood Foliage	Aboveground Very Fast DOM	CO2	CH4	CO	PM25
Softwood Merchantable	0	1							
Softwood Stem Snag		0	0.450			0.477	0.003	0.039	0.010
Medium DOM			0.576			0.298	0.006	0.068	0.017
Softwood Foliage				0	0.00	0.868	0.005	0.070	0.019
Aboveground Very Fast DOM					0.02	0.851	0.005	0.069	0.019
CO2									
CH4									
CO									
PM25									

Table 17. High severity Disturbance Matrix in TSE. Note: only some biomass and atmospheric pools are shown.

	Softwood Merchantable	Softwood Stem Snag	Medium DOM	Softwood Foliage	Aboveground Very Fast DOM	CO2	CH4	CO	PM25
Softwood Merchantable	0	1							
Softwood Stem Snag		0	0.450			0.477	0.003	0.039	0.010
Medium DOM			0.777			0.157	0.003	0.036	0.009
Softwood Foliage				0	0.00	0.868	0.005	0.070	0.019
Aboveground Very Fast DOM					0.05	0.825	0.005	0.066	0.018
CO2									
CH4									
CO									
PM25									

- . This article was produced from an RMarkdown document with underlying data, available at <https://github.com/nrcan-cfs-fire/FireDMs>
- . The authors declare no competing interests.
- . The algorithm and results presented only apply to boreal and temperate forest ecosystems where sufficient ground plots of fire severity are available. As a data-driven model, this framework is not suitable for other ecosystems nor agricultural or forestry biomass burning practices.

References

- Alexander, M. E.: Surface fire spread potential in trembling aspen during summer in the Boreal Forest Region of Canada, *The Forestry Chronicle*, 86, 200–212, <https://doi.org/10.5558/tfc86200-2>, 2010.
- Andreae, M. O.: Emission of trace gases and aerosols from biomass burning – an updated assessment, *Atmospheric Chemistry and Physics*, 19, 8523–8546, [https://doi.org/https://doi.org/10.5194/acp-19-8523-2019](https://doi.org/10.5194/acp-19-8523-2019), 2019.
- Angers, V. A., Gauthier, S., Drapeau, P., Jayen, K., Bergeron, Y., Angers, V. A., Gauthier, S., Drapeau, P., Jayen, K., and Bergeron, Y.: Tree mortality and snag dynamics in North American boreal tree species after a wildfire: a long-term study, *International Journal of Wildland Fire*, 20, 751–763, <https://doi.org/10.1071/WF10010>, publisher: CSIRO PUBLISHING, 2011.
- Barber, Q. E., Jain, P., Whitman, E., Thompson, D. K., Guindon, L., Parks, S. A., Wang, X., Hethcoat, M. G., and Parisien, M.-A.: The Canadian Fire Spread Dataset, *Scientific Data*, 11, 764, <https://doi.org/10.1038/s41597-024-03436-4>, 2024.
- Beilman, D. W., Vitt, D. H., Bhatti, J. S., and Forest, S.: Peat carbon stocks in the southern Mackenzie River Basin: uncertainties revealed in a high-resolution case study, *Global Change Biology*, 14, 1221–1232, <https://doi.org/10.1111/j.1365-2486.2008.01565.x>, 2008.
- Benscoter, B. W., Thompson, D. K., Waddington, J. M., Flannigan, M. D., Wotton, B. M., Groot, W. J. d., and Turetsky, M. R.: Interactive effects of vegetation, soil moisture and bulk density on depth of burning of thick organic soils, *International Journal of Wildland Fire*, 20, 418–429, <https://doi.org/10.1071/WF08183>, 2011.
- Bernier, P. Y., Gauthier, S., Jean, P.-O., Manka, F., Boulanger, Y., Beaudoin, A., and Guindon, L.: Mapping Local Effects of Forest Properties on Fire Risk across Canada, *Forests*, 7, 157, <https://doi.org/10.3390/f7080157>, 2016.
- Binte Shahid, S., Lacey, F. G., Wiedinmyer, C., Yokelson, R. J., and Barsanti, K. C.: NEIVAv1.0: Next-generation Emissions InVentory expansion of Akagi et al. (2011) version 1.0, *Geoscientific Model Development*, 17, 7679–7711, <https://doi.org/10.5194/gmd-17-7679-2024>, 2024.
- Bona, K. A., Shaw, C., Thompson, D. K., Hararuk, O., Webster, K., Zhang, G., Voicu, M., and Kurz, W. A.: The Canadian model for peatlands (CaMP): A peatland carbon model for national greenhouse gas reporting, *Ecological Modelling*, 431, 109 164, <https://doi.org/10.1016/j.ecolmodel.2020.109164>, 2020.
- Bona, K. A., Webster, K. L., Thompson, D. K., Hararuk, O., Zhang, G., and Kurz, W. A.: Using the Canadian Model for Peatlands (CaMP) to examine greenhouse gas emissions and carbon sink strength in Canada's boreal and temperate peatlands, *Ecological Modelling*, 490, 110 633, <https://doi.org/10.1016/j.ecolmodel.2024.110633>, 2024.
- Boulanger, Y., Sirois, L., and Hébert, C.: Fire severity as a determinant factor of the decomposition rate of fire-killed black spruce in the northern boreal forest, *Canadian Journal of Forest Research*, 41, 370–379, <https://doi.org/10.1139/X10-218>, publisher: NRC Research Press, 2011.
- Bourgeau-Chavez, L. L., Grelak, S. L., Billmire, M., Jenkins, L. K., Kasischke, E. S., and Turetsky, M. R.: Mapping Boreal Peatland Fire Severity and Assessing their Potential Vulnerability to Early Season Wildland Fire, *Frontiers in Forests and Global Change*, 3, <https://doi.org/10.3389/ffgc.2020.00020>, 2020.
- Brecka, A. F. J., Boulanger, Y., Searle, E. B., Taylor, A. R., Price, D. T., Zhu, Y., Shahi, C., and Chen, H. Y. H.: Sustainability of Canada's forestry sector may be compromised by impending climate change, *Forest Ecology and Management*, 474, 118 352, <https://doi.org/10.1016/j.foreco.2020.118352>, 2020.
- Brown, J. K. and DeByle, N. V.: Fire damage, mortality, and suckering in aspen, *Canadian Journal of Forest Research*, 17, 1100–1109, <https://doi.org/10.1139/x87-168>, publisher: NRC Research Press, 1987.

- Byrne, B., Liu, J., Bowman, K. W., Pascolini-Campbell, M., Chatterjee, A., Pandey, S., Miyazaki, K., van der Werf, G. R., Wunch, D., Wennberg, P. O., and et al.: Carbon emissions from the 2023 Canadian wildfires, *Nature*, p. 1–5, <https://doi.org/10.1038/s41586-024-07878-z>, 2024.
- Chen, J., Anderson, K., Pavlovic, R., Moran, M. D., Englefield, P., Thompson, D. K., Munoz-Alpizar, R., and Landry, H.: The FireWork v2.0 air quality forecast system with biomass burning emissions from the Canadian Forest Fire Emissions Prediction System v2.03, *Geoscientific Model Development*, 12, 3283–3310, <https://doi.org/10.5194/gmd-12-3283-2019>, 2019.
- Clark, T. L., Radke, L., Coen, J., and Middleton, D.: Analysis of Small-Scale Convective Dynamics in a Crown Fire Using Infrared Video Camera Imagery, *Journal of Applied Meteorology*, 38, 1401–1420, [https://doi.org/10.1175/1520-0450\(1999\)038<1401:AOSSCD>2.0.CO;2](https://doi.org/10.1175/1520-0450(1999)038<1401:AOSSCD>2.0.CO;2), 1999.
- Cocke, A. E., Fulé, P. Z., and Crouse, J. E.: Comparison of burn severity assessments using Differenced Normalized Burn Ratio and ground data, *International Journal of Wildland Fire*, 14, 189–198, <https://doi.org/10.1071/WF04010>, 2005.
- Coen, J. L., Schroeder, W., and Quayle, B.: The Generation and Forecast of Extreme Winds during the Origin and Progression of the 2017 Tubbs Fire, *Atmosphere*, 9, 462, <https://doi.org/10.3390/atmos9120462>, 2018.
- Crutzen, P. J., Heidt, L. E., Krasnec, J. P., Pollock, W. H., and Seiler, W.: Biomass burning as a source of atmospheric gases CO, H₂, N₂O, NO, CH₃Cl and COS, *Nature*, 282, 253–256, <https://doi.org/10.1038/282253a0>, 1979.
- Cumming, S. G.: Effective fire suppression in boreal forests, *Canadian Journal of Forest Research*, 35, 772–786, <https://doi.org/10.1139/x04-174>, publisher: NRC Research Press, 2005.
- Davidson, E. A. and Kanter, D.: Inventories and scenarios of nitrous oxide emissions, *Environmental Research Letters*, 9, 105012, <https://doi.org/10.1088/1748-9326/9/10/105012>, 2014.
- Davies, G. M., Domènech, R., Gray, A., and Johnson, P. C. D.: Vegetation structure and fire weather influence variation in burn severity and fuel consumption during peatland wildfires, *Biogeosciences*, 13, 389–398, <https://doi.org/10.5194/bg-13-389-2016>, 2016.
- de Groot, W., Pritchard, J., and Lynham, T.: Forest floor fuel consumption and carbon emissions in Canadian boreal forest fires, *Canadian Journal of Forest Research*, 39, 367–382, <https://doi.org/10.1139/X08-192>, 2009a.
- de Groot, W., Pritchard, J., and Lynham, T.: Forest floor fuel consumption and carbon emissions in Canadian boreal forest fires, *Canadian Journal of Forest Research*, 39, 367–382, <https://doi.org/10.1139/X08-192>, 2009b.
- de Groot, W., Flannigan, M. D., and Cantin, A. S.: Climate change impacts on future boreal fire regimes, *Forest Ecology and Management*, 294, 35–44, <https://doi.org/10.1016/j.foreco.2012.09.027>, 2013.
- de Groot, W., Hanes, C. C., and Wang, Y.: Crown fuel consumption in Canadian boreal forest fires, *International Journal of Wildland Fire*, <https://doi.org/10.1071/WF21049>, 2022.
- Eidenshink, J., Schwind, B., Brewer, K., Zhu, Z.-L., Quayle, B., and Howard, S.: A Project for Monitoring Trends in Burn Severity, *Fire Ecology*, 3, 3–21, <https://doi.org/10.4996/fireecology.0301003>, 2007.
- Elzhov, T. V., Mullen, K. M., Spiess, A.-N., and Bolker, B.: minpack.lm: R Interface to the Levenberg-Marquardt Nonlinear Least-Squares Algorithm Found in MINPACK, Plus Support for Bounds, <https://cran.r-project.org/web/packages/minpack.lm/index.html>, 2023.
- French, N. H. F., Graham, J., Whitman, E., and Bourgeau-Chavez, L. L.: Quantifying surface severity of the 2014 and 2015 fires in the Great Slave Lake area of Canada, *International Journal of Wildland Fire*, <https://doi.org/10.1071/WF20008>, 2020.
- Gibson, C. M., Chasmer, L. E., Thompson, D. K., Quinton, W. L., Flannigan, M. D., and Olefeldt, D.: Wildfire as a major driver of recent permafrost thaw in boreal peatlands, *Nature Communications*, 9, 1–9, <https://doi.org/10.1038/s41467-018-05457-1>, 2018.

- Gibson, C. M., Estop-Aragonés, C., Flannigan, M., Thompson, D. K., and Olefeldt, D.: Increased deep soil respiration detected despite reduced overall respiration in permafrost peat plateaus following wildfire, *Environmental Research Letters*, 14, 125 001, <https://doi.org/10.1088/1748-9326/ab4f8d>, 2019.
- Griffin, D., Chen, J., Anderson, K., Makar, P., McLinden, C. A., Dammers, E., and Fogal, A.: Biomass burning CO emissions: exploring insights through TROPOMI-derived emissions and emission coefficients, *Atmospheric Chemistry and Physics*, 24, 10 159–10 186, <https://doi.org/10.5194/acp-24-10159-2024>, 2024.
- Group, F. C. F. D. R.: Development and structure of the Canadian Forest Fire Behavior Prediction System, vol. ST-X-3, Forestry Canada, <https://cfs.nrcan.gc.ca/publications?id=10068>, 1992.
- Guindon, L., Bernier, P., Beaudoin, A., Pouliot, D., Villemaire, P., Hall, R., Latifovic, R., and St-Amant, R.: Annual mapping of large forest disturbances across Canada's forests using 250 m MODIS imagery from 2000 to 2011, *Canadian Journal of Forest Research*, 44, 1545–1554, <https://doi.org/10.1139/cjfr-2014-0229>, 2014.
- Guindon, L., Manka, F., Correia, D. L., Villemaire, P., Smiley, B., Bernier, P., Gauthier, S., Beaudoin, A., Boucher, J., and Boulanger, Y.: A new approach for Spatializing the CANadian National Forest Inventory (SCANFI) using Landsat dense time series, *Canadian Journal of Forest Research*, <https://doi.org/10.1139/cjfr-2023-0118>, 2024.
- Hall, R. J., Freeburn, J. T., Groot, W. J. d., Pritchard, J. M., Lynham, T. J., Landry, R., Hall, R. J., Freeburn, J. T., Groot, W. J. d., Pritchard, J. M., and et al.: Remote sensing of burn severity: experience from western Canada boreal fires, *International Journal of Wildland Fire*, 17, 476–489, <https://doi.org/10.1071/WF08013>, 2008a.
- Hall, R. J., Freeburn, J. T., Groot, W. J. d., Pritchard, J. M., Lynham, T. J., Landry, R., Hall, R. J., Freeburn, J. T., Groot, W. J. d., Pritchard, J. M., and et al.: Remote sensing of burn severity: experience from western Canada boreal fires, *International Journal of Wildland Fire*, 17, 476–489, <https://doi.org/10.1071/WF08013>, 2008b.
- Hall, R. J., Skakun, R. S., Metsaranta, J. M., Landry, R., Fraser, R. H., Raymond, D., Gartrell, M., Decker, V., and Little, J.: Generating annual estimates of forest fire disturbance in Canada: the National Burned Area Composite, *International Journal of Wildland Fire*, <https://doi.org/10.1071/WF19201>, 2020.
- Hanes, C. C., Wang, X., Jain, P., Parisien, M.-A., Little, J. M., and Flannigan, M. D.: Fire-regime changes in Canada over the last half century, *Canadian Journal of Forest Research*, 49, 256–269, <https://doi.org/10.1139/cjfr-2018-0293>, 2019.
- Hanes, C. C., Wang, X., Groot, W. J. d., Hanes, C. C., Wang, X., and Groot, W. J. d.: Dead and down woody debris fuel loads in Canadian forests, *International Journal of Wildland Fire*, 30, 871–885, <https://doi.org/10.1071/WF21023>, publisher: CSIRO PUBLISHING, 2021.
- Hanes, C. C., Wotton, M., Woolford, D. G., Martell, D. L., and Flannigan, M.: Mapping organic layer thickness and fuel load of the boreal forest in Alberta, Canada, *Geoderma*, 417, 115 827, <https://doi.org/10.1016/j.geoderma.2022.115827>, 2022.
- Hanes, C. C., Wotton, M., Bourgeau-Chavez, L., Woolford, D. G., Bélair, S., Martell, D., and Flannigan, M. D.: Evaluation of new methods for drought estimation in the Canadian Forest Fire Danger Rating System, *International Journal of Wildland Fire*, <https://doi.org/10.1071/WF22112>, 2023.
- Hayden, K., Li, S.-M., Liggio, J., Wheeler, M., Wentzell, J., Leithead, A., Brickell, P., Mittermeier, R., Oldham, Z., Mihele, C., Staebler, R., Moussa, S., Darlington, A., Steffen, A., Wolde, M., Thompson, D., Chen, J., Griffin, D., Eckert, E., Ditto, J., He, M., and Gentner, D.: Reconciling the total carbon budget for boreal forest wildfire emissions using airborne observations, *Atmospheric Chemistry and Physics Discussions*, pp. 1–62, <https://doi.org/10.5194/acp-2022-245>, publisher: Copernicus GmbH, 2022.
- Hessburg, P. F., Miller, C. L., Parks, S. A., Povak, N. A., Taylor, A. H., Higuera, P. E., Prichard, S. J., North, M. P., Collins, B. M., Hurteau, M. D., Larson, A. J., Allen, C. D., Stephens, S. L., Rivera-Huerta, H., Stevens-Rumann, C. S., Daniels, L. D., Gedalof, Z., Gray, R. W.,

- Kane, V. R., Churchill, D. J., Hagmann, R. K., Spies, T. A., Cansler, C. A., Belote, R. T., Veblen, T. T., Battaglia, M. A., Hoffman, C., Skinner, C. N., Safford, H. D., and Salter, R. B.: Climate, Environment, and Disturbance History Govern Resilience of Western North American Forests, *Frontiers in Ecology and Evolution*, 7, <https://doi.org/10.3389/fevo.2019.00239>, 2019.
- Holden, S. R., Berhe, A. A., and Treseder, K. K.: Decreases in soil moisture and organic matter quality suppress microbial decomposition following a boreal forest fire, *Soil Biology and Biochemistry*, 87, 1–9, <https://doi.org/10.1016/j.soilbio.2015.04.005>, 2015.
- Hood, S. and Lutes, D.: Predicting Post-Fire Tree Mortality for 12 Western US Conifers Using the First Order Fire Effects Model (FOFEM), *Fire Ecology*, 13, 66–84, <https://doi.org/10.4996/fireecology.130290243>, 2017.
- Hornbrook, R. S., Blake, D. R., Diskin, G. S., Fried, A., Fuelberg, H. E., Meinardi, S., Mikoviny, T., Richter, D., Sachse, G. W., Vay, S. A., and et al.: Observations of nonmethane organic compounds during ARCTAS Part 1: Biomass burning emissions and plume enhancements, *Atmospheric Chemistry and Physics*, 11, 11 103–11 130, <https://doi.org/10.5194/acp-11-11103-2011>, 2011.
- Huang, X. and Rein, G.: Downward spread of smouldering peat fire: the role of moisture, density and oxygen supply, *International Journal of Wildland Fire*, 26, 907–918, <https://doi.org/10.1071/WF16198>, 2017.
- Huda, Q., Lyder, D., Collins, M., Schroeder, D., Thompson, D. K., Marshall, G., Leon, A. J., Hidalgo, K., and Hossain, M.: Study of Fuel-Smoke Dynamics in a Prescribed Fire of Boreal Black Spruce Forest through Field-Deployable Micro Sensor Systems, *Fire*, 3, 30, <https://doi.org/10.3390/fire3030030>, 2020.
- Héon, J., Arseneault, D., and Parisien, M.-A.: Resistance of the boreal forest to high burn rates, *Proceedings of the National Academy of Sciences*, 111, 13 888–13 893, <https://doi.org/10.1073/pnas.1409316111>, 2014.
- Jain, P., Barber, Q. E., Taylor, S. W., Whitman, E., Castellanos Acuna, D., Boulanger, Y., Chavardès, R. D., Chen, J., Englefield, P., Flannigan, M., and et al.: Drivers and Impacts of the Record-Breaking 2023 Wildfire Season in Canada, *Nature Communications*, 15, 6764, <https://doi.org/10.1038/s41467-024-51154-7>, 2024.
- Jones, M. W., Kelley, D. I., Burton, C. A., Di Giuseppe, F., Barbosa, M. L. F., Brambleby, E., Hartley, A. J., Lombardi, A., Mataveli, G., McNorton, J. R., and et al.: State of Wildfires 2023–2024, *Earth System Science Data*, 16, 3601–3685, <https://doi.org/10.5194/essd-16-3601-2024>, 2024.
- Kaiser, J. W., Heil, A., Andreae, M. O., Benedetti, A., Chubarova, N., Jones, L., Morcrette, J.-J., Razinger, M., Schultz, M. G., Suttie, M., and et al.: Biomass burning emissions estimated with a global fire assimilation system based on observed fire radiative power, *Biogeosciences*, 9, 527–554, <https://doi.org/10.5194/bg-9-527-2012>, 2012.
- Kasischke, E. S., O'Neill, K. P., French, N. H. F., and Bourgeau-Chavez, L. L.: Controls on Patterns of Biomass Burning in Alaskan Boreal Forests, p. 173–196, Springer, https://doi.org/10.1007/978-0-387-21629-4_10, 2000.
- Key, C. H. and Benson, N. C.: Landscape Assessment (LA), In: Lutes, Duncan C.; Keane, Robert E.; Caratti, John F.; Key, Carl H.; Benson, Nathan C.; Sutherland, Steve; Gangi, Larry J. 2006. FIREMON: Fire effects monitoring and inventory system. Gen. Tech. Rep. RMRS-GTR-164-CD. Fort Collins, CO: U.S. Department of Agriculture, Forest Service, Rocky Mountain Research Station. p. LA-1-55, 164, <https://www.fs.usda.gov/treesearch/pubs/24066>, 2006.
- Kuntzemann, C. E., Whitman, E., Stralberg, D., Parisien, M.-A., Thompson, D. K., and Nielsen, S. E.: Peatlands promote fire refugia in boreal forests of northern Alberta, Canada, *Ecosphere*, 14, e4510, <https://doi.org/10.1002/ecs2.4510>, 2023.
- Kurz, W. A., Apps, M., Banfield, E., and Stinson, G.: Forest carbon accounting at the operational scale, *The Forestry Chronicle*, 78, 672–679, <https://doi.org/10.5558/tfc78672-5>, 2002.

- Kurz, W. A., Dymond, C. C., White, T. M., Stinson, G., Shaw, C. H., Rampley, G. J., Smyth, C., Simpson, B. N., Neilson, E. T., Trofymow, J. A., and et al.: CBM-CFS3: A model of carbon-dynamics in forestry and land-use change implementing IPCC standards, *Ecological Modelling*, 220, 480–504, <https://doi.org/10.1016/j.ecolmodel.2008.10.018>, 2009.
- Letang, D. and de Groot, W.: Forest floor depths and fuel loads in upland Canadian forests, *Canadian Journal of Forest Research*, 42, 1551–1565, <https://doi.org/10.1139/x2012-093>, 2012.
- Linn, R. R., Goodrick, S. L., Brambilla, S., Brown, M. J., Middleton, R. S., O'Brien, J. J., and Hiers, J. K.: QUIC-fire: A fast-running simulation tool for prescribed fire planning, *Environmental Modelling and Software*, 125, 104616, <https://doi.org/10.1016/j.envsoft.2019.104616>, 2020.
- Lobert, J. M., Scharffe, D. H., Hao, W. M., and Crutzen, P. J.: Importance of biomass burning in the atmospheric budgets of nitrogen-containing gases, *Nature*, 346, 552–554, <https://doi.org/10.1038/346552a0>, 1990.
- McAlpine, R. S.: Testing the Effect of Fuel Consumption on Fire Spread Rate, *International Journal of Wildland Fire*, 5, 143–152, <https://doi.org/10.1071/wf9950143>, 1995.
- McRae, D. J., Lynham, T. J., and Frech, R. J.: Understory prescribed burning in red pine and white pine, *The Forestry Chronicle*, 70, 395–401, <https://doi.org/10.5558/tfc70395-4>, 1994.
- McRae, D. J., Stocks, B. J., Mason, J. A., Lynham, T. J., Blake, T. W., and Hanes, C. C.: Influence of ignition type on fire behavior in semi-mature jack pine., *Information Report GLC-X-19*, <http://cfs.nrcan.gc.ca/publications?id=38237>, 2017.
- Melton, J. R., Arora, V. K., Wisernig-Cojoc, E., Seiler, C., Fortier, M., Chan, E., and Teckentrup, L.: CLASSIC v1.0: the open-source community successor to the Canadian Land Surface Scheme (CLASS) and the Canadian Terrestrial Ecosystem Model (CTEM) – Part 1: Model framework and site-level performance, *Geoscientific Model Development*, 13, 2825–2850, <https://doi.org/https://doi.org/10.5194/gmd-13-2825-2020>, 2020.
- Michaletz, S. T. and Johnson, E. A.: A heat transfer model of crown scorch in forest fires, *Canadian Journal of Forest Research*, 36, 2839–2851, <https://doi.org/10.1139/x06-158>, publisher: NRC Research Press, 2006.
- O'donnell, J. A., Harden, J. W., McGuire, A. D., Kanevskiy, M. Z., Jorgenson, M. T., and Xu, X.: The effect of fire and permafrost interactions on soil carbon accumulation in an upland black spruce ecosystem of interior Alaska: implications for post-thaw carbon loss, *Global Change Biology*, 17, 1461–1474, <https://doi.org/10.1111/j.1365-2486.2010.02358.x>, 2011.
- Olivier, J. G. J., Bouwman, A. F., van der Maas, C. W. M., and Berdowski, J. J. M.: Emission database for global atmospheric research (Edgar), *Environmental Monitoring and Assessment*, 31, 93–106, <https://doi.org/10.1007/BF00547184>, 1994.
- Organization, W. M.: Atmospheric ozone 1985 - volume I Assessment of our understanding of the processes controlling its present distribution and change, no. Report No. 16 in Global Ozone Research and Monitoring Project (GORMP), <https://library.wmo.int/records/item/60466-atmospheric-ozone-1985-volume-i>, 1985.
- Parisien, M.-A., Barber, Q. E., Hirsch, K. G., Stockdale, C. A., Erni, S., Wang, X., Arseneault, D., and Parks, S. A.: Fire deficit increases wildfire risk for many communities in the Canadian boreal forest, *Nature Communications*, 11, 1–9, <https://doi.org/10.1038/s41467-020-15961-y>, 2020.
- Parks, S. A., Dillon, G. K., and Miller, C.: A New Metric for Quantifying Burn Severity: The Relativized Burn Ratio, *Remote Sensing*, 6, 1827–1844, <https://doi.org/10.3390/rs6031827>, 2014.
- Parks, S. A., Parisien, M.-A., Miller, C., Holsinger, L. M., and Baggett, L. S.: Fine-scale spatial climate variation and drought mediate the likelihood of reburning, *Ecological Applications*, 28, 573–586, <https://doi.org/10.1002/eap.1671>, 2018.

- Parks, S. A., Holsinger, L. M., Koontz, M. J., Collins, L., Whitman, E., Parisien, M.-A., Loehman, R. A., Barnes, J. L., Bourdon, J.-F., Boucher, J., and et al.: Giving Ecological Meaning to Satellite-Derived Fire Severity Metrics across North American Forests, *Remote Sensing*, 11, 1735, <https://doi.org/10.3390/rs11141735>, 2019.
- Pérez-Izquierdo, L., Clemmensen, K. E., Strengbom, J., Nilsson, M.-C., and Lindahl, B.: Quantification of tree fine roots by real-time PCR, *Plant and Soil*, 440, 593–600, <https://doi.org/10.1007/s11104-019-04096-9>, 2019.
- Santín, C., Doerr, S. H., Preston, C. M., and González-Rodríguez, G.: Pyrogenic organic matter production from wildfires: a missing sink in the global carbon cycle, *Global Change Biology*, 21, 1621–1633, <https://doi.org/10.1111/gcb.12800>, 2015.
- Simon, H., Beck, L., Bhave, P. V., Divita, F., Hsu, Y., Luecken, D., Mobley, J. D., Pouliot, G. A., Reff, A., Sarwar, G., and Strum, M.: The development and uses of EPA's SPECIATE database, *Atmospheric Pollution Research*, 1, 196–206, <https://doi.org/10.5094/APR.2010.026>, 2010.
- Skakun, R., Castilla, G., Metsaranta, J., Whitman, E., Rodrigue, S., Little, J., Groenewegen, K., and Coyle, M.: Extending the National Burned Area Composite Time Series of Wildfires in Canada, *Remote Sensing*, 14, 3050, <https://doi.org/10.3390/rs14133050>, 2022.
- Smyth, C., Xie, S., Zaborniak, T., Fellows, M., Phillips, C., and Kurz, W. A.: Development of a prototype modeling system to estimate the GHG mitigation potential of forest and wildfire management, *MethodsX*, p. 101985, <https://doi.org/10.1016/j.mex.2022.101985>, 2022.
- Smyth, C., Fellows, M., Morken, S., and Magnan, M.: Development of national post-fire restoration system to assess net GHG impacts and salvage biomass availability, *MethodsX*, 13, 102 932, <https://doi.org/10.1016/j.mex.2024.102932>, 2024.
- Stenzel, J. E., Bartowitz, K. J., Hartman, M. D., Lutz, J. A., Kolden, C. A., Smith, A. M. S., Law, B. E., Swanson, M. E., Larson, A. J., Parton, W. J., and et al.: Fixing a snag in carbon emissions estimates from wildfires, *Global Change Biology*, 25, 3985–3994, <https://doi.org/10.1111/gcb.14716>, 2019.
- Stinson, G., Kurz, W. A., Smyth, C. E., Neilson, E. T., Dymond, C. C., Metsaranta, J. M., Boisvenue, C., Rampley, G. J., Li, Q., White, T. M., and et al.: An inventory-based analysis of Canada's managed forest carbon dynamics, 1990 to 2008, *Global Change Biology*, 17, 2227–2244, <https://doi.org/10.1111/j.1365-2486.2010.02369.x>, 2011.
- Stinson, G., Thandi, G., Aitkin, D., Bailey, C., Boyd, J., Colley, M., Fraser, C., Gelhorn, L., Groenewegen, K., Hogg, A., and et al.: A new approach for mapping forest management areas in Canada, *The Forestry Chronicle*, 95, 101–112, <https://doi.org/10.5558/tfc2019-017>, 2019.
- Stocks, B. J., Mason, J. A., Todd, J. B., Bosch, E. M., Wotton, B. M., Amiro, B. D., Flannigan, M. D., Hirsch, K. G., Logan, K. A., Martell, D. L., and et al.: Large forest fires in Canada, 1959–1997, *Journal of Geophysical Research: Atmospheres*, p. FFR 5–12, <https://doi.org/10.1029/2001JD000484>, 2002.
- Stocks, B. J., Alexander, M. E., Wotton, B. M., Stefner, C. N., Flannigan, M. D., Taylor, S. W., Lavoie, N., Mason, J. A., Hartley, G. R., Maffey, M. E., and et al.: Crown fire behaviour in a northern jack pine-black spruce forest, *Canadian Journal of Forest Research*, 34, 1548–1560, <https://doi.org/10.1139/x04-054>, 2004.
- Strong, W. L. and La Roi, G. H.: Root density-soil relationships in selected boreal forests of central Alberta, Canada, *Forest Ecology and Management*, 12, 233–251, [https://doi.org/10.1016/0378-1127\(85\)90093-3](https://doi.org/10.1016/0378-1127(85)90093-3), 1985.
- Talucci, A. C. and Krawchuk, M. A.: Dead forests burning: the influence of beetle outbreaks on fire severity and legacy structure in sub-boreal forests, *Ecosphere*, 10, e02744, <https://doi.org/10.1002/ecs2.2744>, 2019.
- Thompson, D. K., Simpson, B. N., Whitman, E., Barber, Q. E., and Parisien, M.-A.: Peatland Hydrological Dynamics as A Driver of Landscape Connectivity and Fire Activity in the Boreal Plain of Canada, *Forests*, 10, 534, <https://doi.org/10.3390/f10070534>, 2019.

- Trofymow, J. A., Moore, T. R., Titus, B., Prescott, C., Morrison, I., Siltanen, M., Smith, S., Fyles, J., Wein, R., Camiré, C., Duschene, L., Kozak, L., Kranabetter, M., and Visser, S.: Rates of litter decomposition over 6 years in Canadian forests: influence of litter quality and climate, *Canadian Journal of Forest Research*, 32, 789–804, <https://doi.org/10.1139/x01-117>, publisher: NRC Research Press, 2002.
- Turetsky, M. R., Amiro, B. D., Bosch, E., and Bhatti, J. S.: Historical burn area in western Canadian peatlands and its relationship to fire weather indices, *Global Biogeochemical Cycles*, 18, <https://doi.org/10.1029/2004GB002222>, 2004.
- Van Wagner, C. E.: Duff Consumption by Fire in Eastern Pine Stands, *Canadian Journal of Forest Research*, 2, 34–39, <https://doi.org/10.1139/x72-006>, 1972.
- Van Wagner, C. E.: Development and structure of the Canadian Forest Fire Weather Index System, vol. 35, Canadian Forestry Service, <https://cfs.nrcan.gc.ca/publications?id=19927>, 1987.
- Vay, S. A., Choi, Y., Vadrevu, K. P., Blake, D. R., Tyler, S. C., Wisthaler, A., Hecobian, A., Kondo, Y., Diskin, G. S., Sachse, G. W., and et al.: Patterns of CO₂ and radiocarbon across high northern latitudes during International Polar Year 2008, *Journal of Geophysical Research: Atmospheres*, 116, <https://doi.org/10.1029/2011JD015643>, 2011.
- Voshtani, S., Jones, D. B. A., Wunch, D., Pendergrass, D. C., Wennberg, P. O., Pollard, D. F., Morino, I., Ohyama, H., Deutscher, N. M., Hase, F., and et al.: Quantifying CO emissions from boreal wildfires by assimilating TROPOMI and TCCON observations, *EGUphere*, p. 1–60, <https://doi.org/10.5194/egusphere-2025-858>, 2025.
- Walker, X. J., Baltzer, J. L., Cumming, S. G., Day, N. J., Johnstone, J. F., Rogers, B. M., Solvik, K., Turetsky, M. R., and Mack, M. C.: Soil organic layer combustion in boreal black spruce and jack pine stands of the Northwest Territories, Canada, *International Journal of Wildland Fire*, 27, 125, <https://doi.org/10.1071/WF17095>, 2018a.
- Walker, X. J., Rogers, B. M., Baltzer, J. L., Cumming, S. G., Day, N. J., Goetz, S. J., Johnstone, J. F., Schuur, E. A. G., Turetsky, M. R., and Mack, M. C.: Cross-scale controls on carbon emissions from boreal forest megafires, *Global Change Biology*, 24, 4251–4265, <https://doi.org/10.1111/gcb.14287>, 2018b.
- Walker, X. J., Baltzer, J. L., Bourgeau-Chavez, L. L., Day, N. J., De Groot, W., Dieleman, C., Hoy, E. E., Johnstone, J. F., Kane, E. S., Parisien, M. A., and et al.: ABoVE: Synthesis of Burned and Unburned Forest Site Data, AK and Canada, 1983–2016, ORNL DAAC, <https://doi.org/10.3334/ORNLDAAC/1744>, 2020a.
- Walker, X. J., Rogers, B. M., Veraverbeke, S., Johnstone, J. F., Baltzer, J. L., Barrett, K., Bourgeau-Chavez, L., Day, N. J., de Groot, W. J., Dieleman, C. M., and et al.: Fuel availability not fire weather controls boreal wildfire severity and carbon emissions, *Nature Climate Change*, p. 1–7, <https://doi.org/10.1038/s41558-020-00920-8>, 2020b.
- Wang, X., Oliver, J., Swystun, T., Hanes, C. C., Erni, S., and Flannigan, M. D.: Critical fire weather conditions during active fire spread days in Canada, *Science of The Total Environment*, p. 161831, <https://doi.org/10.1016/j.scitotenv.2023.161831>, 2023.
- White, J. C., Wulder, M. A., Hermosilla, T., Coops, N. C., and Hobart, G. W.: A nationwide annual characterization of 25 years of forest disturbance and recovery for Canada using Landsat time series, *Remote Sensing of Environment*, 194, 303–321, <https://doi.org/10.1016/j.rse.2017.03.035>, 2017.
- Whitman, E., Parisien, M.-A., Thompson, D. K., Hall, R. J., Skakun, R. S., and Flannigan, M. D.: Variability and drivers of burn severity in the northwestern Canadian boreal forest, *Ecosphere*, 9, e02128, <https://doi.org/10.1002/ecs2.2128>, 2018.
- Whitman, E., Parisien, M.-A., Holsinger, L. M., Park, J., and Parks, S. A.: A method for creating a burn severity atlas: an example from Alberta, Canada, *International Journal of Wildland Fire*, <https://doi.org/10.1071/WF19177>, 2020.

Whitman, E., Barber, Q. E., Jain, P., Parks, S. A., Guindon, L., Thompson, D. K., and Parisien, M.-A.: A modest increase in fire weather overcomes resistance to fire spread in recently burned boreal forests, *Global Change Biology*, 30, e17363, <https://doi.org/10.1111/gcb.17363>, 2024.

Wotton, B. M., Gould, J. S., McCaw, W. L., Cheney, N. P., and Taylor, S. W.: Flame temperature and residence time of fires in dry eucalypt forest, *International Journal of Wildland Fire*, 21, 270–281, <https://doi.org/10.1071/WF10127>, 2011.